OXFORD UNIVERSITY PRESS | Systematic Biology

A framework for resolving cryptic species: a case study from the lizards of the Australian Wet Tropics

Journal:	*Systematic Biology*
Manuscript ID	USYB-2017-228.R1
Manuscript Type:	Regular Manuscript
Date Submitted by the Author:	n/a
Complete List of Authors:	Singhal, Sonal; CSU Dominguez Hills, Biology Hoskin, Conrad; James Cook University Faculty of Science and Engineering Couper, Patrick; Queensland Museum, Biodiversity Program Potter, Sally; Australian National University, Research School of Biology Moritz, Craig; Australian National University, Research School of Biology
Keywords:	cryptic species, species delimitation, squamates, phylogeography, exome capture, taxonomy

A framework for resolving cryptic species: a case study from the lizards of the Australian Wet Tropics

Sonal Singhal[1,2], Conrad J. Hoskin[3], Patrick Couper[4], Sally Potter[5], Craig Moritz[5]

[1]Museum of Zoology and Department of Ecology and Evolutionary Biology, University of Michigan, Ann Arbor, MI 48109

[2]Department of Biology, California State University - Dominguez Hills, Carson, CA 90747

[3]College of Science & Engineering, James Cook University, Townsville, Queensland, 4811, Australia

[4]Biodiversity Program, Queensland Museum, South Brisbane, Queensland, 4101, Australia

[5]Division of Ecology and Evolution, Research School of Biology and Centre for Biodiversity Analysis, Australian National University, Acton, ACT, Australia

corresponding author: sonal.singhal1@gmail.com

ABSTRACT

As we collect range-wide genetic data for morphologically-defined species, we increasingly unearth evidence for cryptic diversity. Delimiting this cryptic diversity is challenging, both because the divergences span a continuum and because the lack of overt morphological differentiation suggests divergence has proceeded heterogeneously. Here, we address these challenges as we diagnose and describe species in three co-occurring species groups of Australian lizards. By integrating genomic and morphological data with data on hybridization

and introgression from contact zones, we explore several approaches – and their relative benefits and weaknesses – for testing the validity of cryptic lineages. More generally, we advocate that genetic delimitations of cryptic diversity must consider whether these lineages are likely to be durable and persistent through evolutionary time.

KEYWORDS

cryptic species, species delimitation, squamates, phylogeography, exome capture, taxonomy

INTRODUCTION

Cryptic species, that is taxa that are morphologically similar but genetically divergent, exemplify the two major challenges of species delimitation. First, species form on a continuum (Darwin 1859; Mayr 1942; Mallet 1995; De Queiroz 2007). As populations differentiate across space and time, they gradually become more divergent. As reflected in the debate over defining operational taxonomic units via DNA barcoding (Moritz and Cicero 2004), deciding how much divergence is sufficient to name lineages as species can be arbitrary. As with morphologically distinct lineages, diagnosing cryptic lineages presents this challenge because they fall through the full range of the divergence continuum (Hedgecock and Ayala 1974; Gómez et al. 2002; McDaniel and Shaw 2003). Second, speciation proceeds heterogeneously across many axes. We typically recover correlations across axes – e.g., rates of trait evolution such as song and mitochondrial divergence (Winger and Bates 2015). However, when axes of differentiation are discordant – for example, when phenotypic disparity is high and genetic divergence is low, the status of lineages becomes ambiguous. By definition, cryptic lineages have diverged

heterogeneously (Bickford et al. 2007)—they are genetically-distinct groups that exhibit little or no morphological divergence. The taxonomic process of naming a species is a binary exercise—either a lineage is recognized as a species or not—and accounting for heterogeneity in this binary framework remains a challenge.

Biodiversity researchers increasingly face these challenges because we are increasingly discovering new cryptic lineages (Bickford et al. 2007). A confluence in genetic advances and broader geographic sampling has led to rapid increases in the number of cryptic species, such that a quarter of papers published in Zoological Record Plus mention cryptic species ((Bickford et al. 2007) see also (de León and Poulin 2016)). Cryptic species comprise a significant proportion of the diversity in some regions (e.g., tropics; (Smith et al. 2008)) and taxonomic groups (e.g., reptiles; (Oliver et al. 2010)), and recently, putative cryptic species have been identified in high-profile threatened species like orangutans (Nater et al. 2017). These findings, and their implications for evolutionary biology and conservation (Frankham et al. 2012), emphasize the need for a more rigorous framework to assess the taxonomic status of cryptic lineages (Adams et al. 2014; Struck et al. in press).

In this work, we propose a framework that diagnoses those cryptic lineages that are expected to be sufficiently durable to contribute to build-up of diversity over time and space. Because speciation is a continuum, we expect that many nascent species are lost to hybridization and extinction as part of the protracted speciation process (Rosindell et al. 2010; Dynesius and Jansson 2014). As such, we adopt the biological species concept (BSC, (Mayr 1942)), which defines species as units that exhibit barriers to reproduction and are thus more likely to persist through time. Although some might find this definition overly restrictive, we

apply it here in hopes of avoiding "taxonomic over-inflation" (Isaac et al. 2004). However, how do we diagnose populations that are likely to have substantial reproductive isolation (RI)? In allopatry, the degree of morphological difference is expected to correlate with the extent of RI (Mayr 1942; Bolnick et al. 2006; Funk et al. 2006). Thus, when genetic and phenotypic divergence concur, species delimitation is typically uncontroversial. For cryptic species, where we cannot use phenotypic divergence as a proxy for RI, we must instead use multiple lines of evidence to assess likelihood of strong RI.

A popular approach to assess cryptic lineages is to apply statistical species delimitation to multilocus genetic data (Fujita et al. 2012; Carstens et al. 2013), which some argue makes species delimitation more objective (Rannala 2015). An illuminating line of research has explored the parameter space under which these coalescent-based methods are expected to return statistically robust results (Zhang et al. 2011; Olave et al. 2014). What remains to be seen is if these statistically robust lineages are also biologically robust (Sukumaran and Knowles 2017). That is, will newly delimited lineages remain distinct through changing geographies and environments, or will they be mere evolutionary ephemera lost to hybridization and/or extinction (Seehausen et al. 2008; Rosenblum et al. 2012; Dynesius and Jansson 2014)?

A stronger and more direct approach to delimitation is to test for strongly restricted gene flow in sympatry or parapatry (Richardson et al. 1986; Adams et al. 2014). This can be done either by sampling a modest number of individuals in sympatry or by assessing the extent of genetic introgression through intensive analysis of contact zones between parapatric taxa. However, when candidate taxa are allopatric, assessing the likelihood of strong RI is even more challenging, as long recognized under operational versions of the BSC. To the extent that RI is

time-dependent (Coyne and Orr 1989; Sasa et al. 1998; Fitzpatrick 2002; Roux et al. 2016), another approach is to extrapolate from closely-related taxa where the relationship between divergence and extent of RI has already been determined. In contrast to a "bar-coding gap" (Hebert et al. 2004b), this approach uses genome-scale evidence to assess the likelihood of strong RI rather than patterns of genetic divergence across nominal species vs. populations.

We explore these multiple approaches to species delimitation through the study of morphologically cryptic, phylogeographic lineages in the lizards of the Australian Wet Tropics (AWT). The AWT is a narrow region of rainforest in northeast Queensland, Australia (Fig. 1). During repeated glacial cycles in the Quaternary (Graham et al. 2006), the rainforest and, accordingly, the species endemic to these rainforests, were split across two major refugia. Populations of these rainforest species diverged across these refugia; comparative data have recovered deep phylogeographic splits within species across more than twenty taxa (Moritz et al. 2009). Morphological analyses show limited phenotypic divergence among phylogeographic lineages (Schneider and Moritz 1999; Hoskin et al. 2005; Hoskin et al. 2011). Subsequent contact zone studies showed that some of these phylogeographic lineages are reproductively isolated (Phillips et al. 2004; Hoskin et al. 2005; Singhal and Moritz 2013).

Here, we focus on three species groups—the '*Carlia rubrigularis*', '*Lampropholis coggeri*', and '*Lampropholis robertsi*' groups—which are part of the broader radiation of Eugongylus lizards (family: Scincidae) (Skinner et al. 2011). These groups are ecologically-similar; all are small (30–55 mm) skinks of the leaf-litter in the rainforests of the AWT. Previous multilocus analyses revealed several phylogeographic lineages within each of these nominal taxa (Dolman and Moritz 2006; Bell et al. 2010). Like many phylogeographic units, these lineages are mostly

morphologically cryptic and geographically circumscribed, and their ranges are either geographically proximate or narrowly overlapping. With an eye to integrative taxonomy (Padial et al. 2010), we synthesize data on genetics, morphology, and reproductive isolation assessed in contact zones to resolve the species status of lineages within these three groups and to formally revise their taxonomy. More generally, we use these lizards as a data-rich case study to explore the challenges of delimiting species among cryptic lineages that are parapatric or allopatric.

METHODS

Sampling, Data Collection, and Data Processing

In this study, we analyze genetic data for individuals across three species groups across five nominal species and 13 putative lineages. The '*Carlia rubrigularis*' group consists of five lineages: *C. rubrigularis*, northern Wet Tropics (N); *C. rubrigularis*, southern Wet Tropics (S); *C. rhomboidalis*, northern mid-east Queensland (N); *C. rhomboidalis*, southern mid-east Queensland (S); and *C. wundalthini* at Cape Melville (Fig. 1). The '*Lampropholis coggeri*' group consists of four lineages: *L. coggeri*, northern Wet Tropics (N); *L. coggeri*, central Wet Tropics (C); *L. coggeri*, southern Wet Tropics (S); and *L. coggeri* in the Mt Elliot uplands (EU). The montane '*Lampropholis robertsi*' group consists of four allopatric lineages: *L. robertsi*, Carbine Tableland uplands (CU); *L. robertsi*, Thornton Peak uplands (TU); *L. robertsi*, Mt Bellenden Ker (BK); and *L. robertsi*, Mt Bartle Frere and southern Atherton Tablelands (BFAU).

These lineages had been previously described through the sequencing of an average of 27 geographically dispersed individuals per lineage for mtDNA and 12 for multi-locus nDNA

(Dolman and Moritz 2006; Bell et al. 2010). Because these lineages were sampled extensively in previous genetic analyses and because they are circumscribed geographically (Fig. 1), we limited our sampling to a few individuals per lineage (Fig. 1; Table S1-2). Further, across these lineages, three lineage-pairs meet in hybrid zones, two of which are very narrow (<1 km) and the other of which is wider (<10 km) (Singhal & Moritz 2013; Singhal & Bi 2017). Given that introgression is geographically limited relative to lineage ranges, we selected individuals well removed from contemporary contact zones to estimate species trees, test for lineage-wide introgression, and to apply statistical delimitation methods. We further included two outgroups: *C. storri* for the '*C. rubrigularis*' group and *L. amicula* for the '*L. coggeri*' and '*L. robertsi*' groups. For *L. coggeri* N and C, we supplemented our sampling by including previously-published transcriptome data (Singhal 2013), which we analyzed using the same approach outlined below. In total, we sampled 25 individuals (Table S1-2).

We sequenced a homologous set of 3320 loci across all individuals using an exome capture approach previously described (Bragg et al. 2016). Briefly, we identified homologous exons across the Eugongylus skink clade from transcriptome data of three species. After filtering the exons for GC-content and length, we included probes specific to each of the three species in the capture array. For each sample, we extracted DNA (Sunnucks and Hales 1996) and generated uniquely-barcoded libraries (Meyer and Kircher 2010). Individuals were then pooled in equimolar amounts along with other Eugongylus group taxa (Bragg et al. 2018), and we captured our target exons using a SeqCap EZ Developer Probes following manufacturer's instructions. The captured libraries were subsequently sequenced along with samples for other projects on the Illumina HiSeq2000 and 2500 for 100 bp paired-end reads.

Our bioinformatics pipeline is designed for both population genetic and phylogenetic analyses and thus generates both variant data for each lineage and locus alignments across all haplotypes in a given group. The basic approach follows, with further details available in Singhal et al. (2017). Following de-multiplexing, we trimmed low quality sequence and adaptor sequence from reads using TRIMMOMATIC v0.36 and merged overlapping reads using PEAR v0.9.10 (Zhang et al. 2013; Bolger et al. 2014). We generated an assembly for each individual with TRINITY v2.3.2 and identified assembled contigs homologous to our original targets with BLAT v36x1 (Kent 2002; Grabherr et al. 2011). For each exon, we picked the best matching contig across all individuals in the lineage to generate a pseudo-reference genome. We then annotated the coding sequence for these exons using EXONERATE v2.2.0 (Slater and Birney 2005). To generate variant data, we mapped reads from each individual to the pseudo-reference genome using BWA v0.7.12 (Li and Durbin 2009), called variant and invariant sites using GATK v3.6 UNIFIEDGENOTYPER, filtered out sites with quality <20, quality depth (QD) <5, and coverage <20×, and then determined haplotypes using GATK READBACKEDPHASING (McKenna et al. 2010). Eight percent of sites were unphased; for these sites, we randomly phased them with respect to other phased blocks. We then generated multi-lineage alignments across all haplotypes with MAFFT v7.294 (Katoh et al. 2002).

Like many phylogeographic studies, we first identified these lineages by sequencing mitochondrial loci. For these taxa, mtDNA and nDNA are highly congruent except within narrow contact zones, and mtDNA provides our most complete understanding of geographic limits (Dolman and Moritz 2006; Bell et al. 2010). Accordingly, we downloaded all geo-

referenced *NADH dehydrogenase subunit 4* (ND4) data for these groups from GenBank (Table S3). We aligned the data using MAFFT and identified the coding sequence using EXONERATE.

Phylogenetic Analyses

We reconstructed the evolutionary history of 13 lineages and two outgroups by using STARBEAST2 v0.13.5, a coalescent multi-locus method (Ogilvie et al. 2017). Individuals were assigned to lineages following their 'putative lineage' designations (Table S2). We filtered loci to only include those that were ≥75% complete across samples and to remove loci ≥1500 bp because longer loci are more likely to capture recombination events. Because of the computational demands of running STARBEAST2, we generated three random subsamples of 200 loci each from the remaining loci. We ran STARBEAST2 on these random subsets for 500e6 generations sampling every 1e5 generations. Each locus was assigned to its own strict clock and a GTR model of molecular evolution. Because we lack robust age constraints for nodes in this species tree, we instead inferred branch lengths in units of substitutions per site.

For the mitochondrial phylogenetic analysis, we determined the best-fitting partitioning strategy using PARTITIONFINDER2 (Lanfear et al. 2016). We then inferred the mtDNA gene trees using MRBAYES v3.2.6, running 2 runs of 4 chains each for 50e6 steps (Ronquist et al. 2012). We set the branch length prior to exponential(100); the default prior overestimates branch lengths when the majority of bifurcations occur within-species (Brown et al. 2009).

Population Genetic Analyses

Our population genetic analyses were aimed at describing basic patterns of diversity, divergence, and current and historical introgression among the lineages in these groups. For each lineage, we calculated within-lineage genetic diversity (π; (Nei and Li 1979)) for both the exome and mtDNA data, across silent sites only. For each pairwise-comparison between lineages in a species group, we calculated raw and net divergence (d_{xy} and d_a) for the exome and mtDNA data (Nei and Li 1979), again across silent sites only. The patterns of divergence and diversity among individuals within a lineage and across lineages confirm our lineage assignments based on mtDNA and previous multilocus nuclear data (Dolman and Moritz 2006; Bell et al. 2010).

To test for historical introgression, we used the D-statistic (Durand et al. 2011). For the topology ((P1, P2), P3), outgroup), the D-statistic distinguishes if P1 and P3 exhibit incomplete lineage sorting or introgression by comparing site patterns across these four tips. We conducted this test across all possible comparisons within species groups, except for sister taxa, which cannot be accommodated in the D-statistic framework. Based on overall species tree topology (Fig. 2), we determined the appropriate species to use as P2 (Table S5). For all *Lampropholis* comparisons, we used *L. amicula* as the outgroup, and for *Carlia,* we used *C. storri*. Because of our limited within-lineage sampling, we implemented the version of the test designed for fixed variants. Thus, we removed any site that was missing or polymorphic for any lineage in a species group. For the remaining sites, we calculated the D-statistic across all possible species comparisons. To assess significance, we calculated the standard deviation across 200 bootstraps and used a one-tailed z-test (Eaton and Ree 2013). For *L. robertsi*, we further tested for introgression using the D_{FOIL} approach designed for five-taxon symmetric

topologies (Pease and Hahn 2015); we could not apply this method to other groups because their topologies are asymmetric. This method confirmed our D-statistic results, so we do not discuss them further.

Finally, we collated previously-published data on reproductive isolation at three contact zones: *L. coggeri* N and C, *L. coggeri* C and S, and *C. rubrigularis* N and S (Phillips et al. 2004; Dolman 2008; Singhal and Moritz 2012, 2013; Singhal and Bi 2017). These studies sampled densely through each contact zone to infer current rates of hybridization and to determine patterns of introgression across the genome and geography.

Statistical Species Delimitation

One of the most common ways to validate cryptic lineages is through multilocus coalescent-based (MSC) approaches (Fujita et al. 2012). Accordingly, and as recommended by Rannala (2015), we used two MSC approaches (BPP v3.3a and STACEY v1.2.4) to test species boundaries across these groups (Yang and Rannala 2014; Jones 2017). Using the same filtering as in our STARBEAST2 analyses, we selected three random samples of 100 loci per species group and generated input files for BPP and STACEY. We used the species tree inferred from the STARBEAST2 analyses (see *Phylogenetic Analyses*) as the guide tree for BPP. For the *'L. coggeri'* group, we used two topologies of the species tree that reflected uncertainty in the placement of *L. coggeri* EU (Fig. S1). We then ran BPP for 500,000 generations across three sets of priors to ensure our results were robust to prior specification. These priors were: (1) θ~(2, 2000), τ~(2, 2000), (2) θ ~(1, 10), τ ~(1, 10), and (3) θ ~(1, 10), τ ~(2, 2000). We ensured that we had 20 – 80% acceptance rate; having too high or too low of acceptance rates can affect results. We ran

241 STACEY for 1e7 generations. Each locus was set to have its own clock rate and own substitution
242 model under a HKY model. Priors were: collapse height = 0.001, growth rate ~
243 lognormal(mean=5, sd=2); collapse weight ~ uniform(0,1); population prior scale ~
244 lognormal(mean=-7,sd=2), and relative death rate ~ β (α=1, β=8). Species delimitations were
245 determined using SPECIESDA with a burn-in of 10% and a collapse height of 0.0001 (Jones 2017).
246 Analyses showed that results were robust across collapse heights from 0.0001 to 0.001.
247
248 *Morphological Data and Analysis*
249 We assessed morphological differences in scale and body measurement traits between the major
250 genetic lineages in each of the three species groups in the Wet Tropics region. For the '*C.*
251 *rubrigularis'* species group, we excluded *C. wundalthini* and *C. rhomboidalis* because they differ in
252 breeding colors and to some degree body size and shape (Dolman 2008; Hoskin 2014). Further,
253 we combined individuals from *L. coggeri* N and C, from *L. robertsi* CU and TU, and *L. robertsi* BK
254 and BFAU because our analyses of the genomic evidence suggested these lineages are not
255 distinct and should be collapsed (see the *Discussion*). A single investigator took scale counts and
256 body measurements on an average of 26 specimens per lineage (Appendix 1, Table S4). The
257 traits measured summarize morphological characteristics that affect how lizards function in
258 their environment (e.g., relative limb length affects locomotion; (Losos 2011)) and are
259 standardly used to delimit skink species (Ingram and Covacevich 1989; Ingram 1991; Greer
260 1997).
261 The scale traits counted were the number of supraciliaries, infralabials, supralabials,
262 midbody scale rows, paravertebrals, and lamellae under the fourth toe (Hoskin 2014). We found

no to little variation for these scale traits within species groups and thus performed no further analyses (Table A4). We measured five aspects of body size and shape: total head and body length (snout to vent length, SVL), distance between the front and hindlimbs (axilla to groin length, AG), length of the hindlimb (L2), head length (HL), and head width (HW) (Hoskin 2014). Only adults were measured, defined as individuals with SVL greater than 48 mm, 44 mm, and 32 mm in *C. rubrigularis*, *L. robertsi*, and *L. coggeri* respectively.

For each species group, we used multivariate analyses to determine if lineages differed significantly in size or shape. We first used a principal component analysis (PCA) to summarize across all five body measurements (Jolliffe 2002). We then tested if body size (PC1) and body shape (PCs 2–5) varied significantly across lineages. All analyses were nested by region within lineage to account for among-region variation within lineages. 'Region' represents different mountain ranges, tablelands, and lowland areas, and roughly matched the subregions defined for the Wet Tropics (Bell et al. 2010). For body size, we used a nested univariate analysis of variance (ANOVAs) of PC1 between lineages within each species group. For body shape, we used a nested multivariate analysis of variance (MANOVA) of PCs 2–5. Significance was assessed using Roy's Greatest Root. For those species groups where we included more than two lineages, we performed nested univariate (size) or multivariate (shape) planned contrasts to test which lineages differed significantly. All analyses were conducted in SAS v9.2.

RESULTS

Analysis of Genetic Data

Our exome capture approach worked well across all lineages. On average, we recovered an average of 2.29 Mb per individual across 2668 loci at an average coverage of 112× (Table S2).

The inferred topology is well-supported and is consistent with previous phylogenetic hypotheses based on mtDNA data (Fig. 2, Fig. S2; (Bell et al. 2010)) and other phylogenomic analyses (Bragg et al. 2018). Branching times and topologies were quantitatively and qualitatively similar across replicate analyses of STARBEAST2 (Fig. S1). The branching times between these lineages all occur within a narrow range and highlight that two lineages of *C. rubrigularis* as currently recognized are polyphyletic. Further, the splitting patterns generally agree with the biogeographic relationships between species. For example, *L. robertsi* BFAU is sister to *L. robertsi* BK, and the two lineages occur as adjacent montane isolates (Fig. 1, Fig. 2). The exception to this congruence is a leapfrog distribution of *L. coggeri* EU, which is sister to *L. coggeri* N and C rather than the geographically adjacent *L. coggeri* S (Fig. 1, Fig. 2).

We inferred a ~4×-9× range of genetic divergences between lineages within nominal species, with nuclear d_{xy} at silent sites ranging from 0.5% - 1.95% and nuclear d_a ranging from 0.18% - 1.68% (Fig. 3, Table S5). Lineages associated with small ranges such as *C. wundalthini* and the montane lineages of *L. robertsi* showed lower levels of within-population diversity. Measures of mtDNA and nuclear d_{xy} and d_a were correlated (d_{xy}; r = 0.61, p-value =0.016; d_a; r = 0.57, p-value=0.025; Fig. 3A-B). As for inferred branching times, divergences between some cryptic lineages were significantly greater than those between nominal species (Fig. 3C).

Our D-statistic tests for historical introgression among non-sister lineages recovered four likely cases of historical introgression between lineage-pairs: *C. rubrigularis* N and S; *C. rubrigularis* N and *C. rhomboidalis*; *L. coggeri* S and EU; and *L. coggeri* C and S (Fig. 2, Table S6).

No signature of historical introgression was recovered for strongly allopatric populations – e.g., among montane isolates of the '*L. robertsi*' species group, and *C. wundalthini* vs. *C. rubrigularis*. Our previous results from analyses of hybridization and introgression at contact zones show that *C. rubrigularis* N and S and *L. coggeri* C and S exhibit (1) a moderate proportion of hybrids in the center of the contact zones, (2) narrow cline widths across the genome, and (3) auto-correlation in cline widths across physical distances, all indicative of extensive disequilibrium in hybrids and substantial RI (Fig. 4). The less divergent lineage-pair, *L. coggeri* N and C, shows none of the same patterns, with evidence of extensive introgression across the genome and geography.

Statistical species delimitation supported all lineages as species. BPP returned ≥95% probability for a speciation event at all nodes in our guide trees, and STACEY inferred each species as a unique cluster (Fig. 2). This result was robust to priors and, for the '*L. coggeri*' group, uncertainty in the topology.

Analysis of Morphological Data

For all three species groups, PCAs resulted in a PC1 that accounted for most of the variation (67–84%). It was loaded highly and positively by all body measurements and indicated body size (Tables S7–9). The remaining four PCs in each species group represented variation in body shape (Tables S7-9). PC2 accounted for 10–16% of the variation in the species groups, and was loaded most heavily by relative AG length (positive) in '*C. rubrigularis*' and both AG length (positive) and relative L2 length (negative) in *'L. robertsi*' and *'L. coggeri*' (Tables S7-9).

The three major lineages in the *'L. coggeri'* group show no differences in body size ('lineage' effect on PC1, $F_{2,58} = 2.46$, P = 0.09), but they do differ in body shape ('lineage' effect on PC2–5, Wilks' Lambda $F_{8,10} = 3.46$, P = 0.04) (Fig. 5B, Table 1). This significant variance was driven by CV1 (Roy's Greatest Root $F_{4,6} = 6.05$, P = 0.03), which is loaded most heavily by PC2 (0.489; Table S10). Multivariate contrasts revealed that only *L. coggeri* EU and S differ significantly in shape ($F_{4,5} = 5.00$, P = 0.05) (Table 1). Neither *L. coggeri* EU and N/C ($F_{4,5} = 3.35$, P = 0.11) nor *L. coggeri* N/C and S ($F_{4,5} = 2.56$, P = 0.17) differed in shape. Therefore, the only detectible difference was that *L. coggeri* EU has a relatively longer body and shorter legs than the geographically adjacent, but distantly related, *L. coggeri* S.

No morphological differences were detected between the N and S lineages of '*C. rubrigularis*', for either body size ('lineage' effect on PC1, $F_{1,50} = 1.17$, P = 0.29) or body shape ('lineage' effect on PC2–5, Wilks' Lambda $F_{4,5} = 0.45$, P = 0.77) (Fig. 5A, Table 1). Similarly, no significant differences were detected between the TU/CU and BK/BFAU lineages of *'L. robertsi'*. Body size was marginally non-significant ('lineage' effect on PC1, $F_{1,28} = 3.89$, P = 0.06), and body shape did not differ ('lineage' effect on PC2–5, Wilks' Lambda $F_{3,1} = 2.68$, P = 0.42) (Fig. 5C, Table 1).

DISCUSSION

Delimitation of cryptic species

Initial phylogeographic explorations based on mtDNA revealed that each species group contained at least four to five lineages, most of which were deeply divergent. Subsequent sequencing of five to ten nuclear loci confirmed that these phylogeographic lineages were also

diverged at the nuclear genome (Dolman and Moritz 2006; Bell et al. 2010). Now, genetic data based on over 2500 exons confirmed that these lineages exhibit genetic divergences of substantial but varying depths. These genetic divergences all fall within the range that comparative data suggest spans the transition from populations to isolated species (Roux et al. 2016). Although some of the lineages are far more divergent than some already recognized species, and although we focused on morphological traits standardly used in lizard taxonomy and eco-evolutionary studies (Ingram 1991; Losos 2011; Hoskin 2014), we found little or no morphological divergence between the major lineages within each of the three species groups. Accordingly, these can mostly regarded as truly cryptic, rather than pseudo-cryptic, species.

Given morphologically cryptic lineages that span a range of divergences, and all of which are delimited using coalescent methods, we are thus faced with the two challenges of species delimitation: how to determine how much genetic divergence is sufficient when divergences are arrayed on a continuum; and how to reconcile when genetic and phenotypic data give conflicting perspectives. As a first step, we can directly assess levels of isolation between these lineages because three of the lineage-pairs in these groups meet in narrow zones of parapatry (Fig. 4).

Through these fine-scale contact zone analyses of isolation, we have two major findings. First, we find that, like genetic divergence, RI exists on a continuum, with lineages exhibiting varying degrees of isolation (Fig. 4A–B). For this set of lineages, divergence and isolation appear to scale, although non-linearly. The average cline width at the *L. coggeri* C and S hybrid zone zone is about 5.5× less than that at the *L. coggeri* N and C contact. Yet, *L. coggeri* C and S is only 1.6× more genetically divergent than *L. coggeri* N and C. Theory does not predict a linear scaling;

372 the cline width of a locus is proportional to the inverse square root of selection on that locus
373 (Barton and Gale 1993). Thus, as selection on a locus increases, cline width can sharpen
374 narrowly and quickly, as seen here. Further evidence of this non-linear accumulation of RI can
375 be seen in patterns of linkage disequilibrium in these contact zones. Data from *L. coggeri* N and
376 C show no evidence for disequilibrium at introgressing sites, whereas *C. rubrigularis* N and S
377 and *L. coggeri* C and S exhibit extensive disequilibrium extending a few kilobases (Fig. 4C).
378 These results confirm theoretical expectations that lineages can quickly transition from acting as
379 populations (*i.e.*, *L. coggeri* N and C) to acting as genomically isolated species (*i.e.*, *L. coggeri* C
380 and S and *C. rubrigularis* N and S) (Turner 1967; Barton 1983).
381 Second, these data show that, despite being nearly identical morphologically, the more
382 genetically divergent lineages have substantial RI. At least for *C. rubrigularis* N and S, these
383 lineages are not isolated by premating isolation (Dolman 2008), but rather by post-mating
384 selection against hybrids (Phillips et al. 2004). Based on estimates of dispersal length and cline
385 width of the hybrid index, selection against hybrids is strong. Hybrids between *C. rubrigularis* N
386 and S and *L. coggeri* C and S are estimated to be 50-70% and 10-65% less fit than their parents,
387 respectively (Phillips et al. 2004; Singhal and Moritz 2012). Estimated selection on hybrids
388 between *L. coggeri* N and C, on the other hand, is negligible. The selection against hybrids seen
389 in *C. rubrigularis* N and S and *L. coggeri* C and S is comparable (if not greater) than that seen
390 between morphologically distinct hybridizing taxon-pairs. (Barton and Gale 1993; Singhal and
391 Moritz 2012). Such strong selection suggests that these lineages will remain evolutionary
392 distinct in the future, despite the high potential for gene flow. As such, we propose to identify
393 *C. rubrigularis* N and S as separate species, and likewise for *L. coggeri* S and *L. coggeri* C. Because

394 we found no evidence for RI between *L. coggeri* N and C, we retain them as distinct populations
395 within one species (*L. coggeri* N/C).
396 However, how should we diagnose those lineages for which we cannot indirectly or
397 directly assay RI? For example, *L. coggeri* EU is geographically isolated from *L. coggeri* N/C and
398 S, and the lineages in the '*L. robertsi*' group are isolated on different mountaintops. These
399 lineages do not meet in contact zones, and because of both practical and ethical reasons, cannot
400 be easily kept in the laboratory for experimental trials. Instead, we extrapolate our estimates of
401 RI from the three lineage-pairs that do meet in parapatry (Fig. 4) to the species group as a
402 whole. This extrapolation assumes that the tempo and mode at which RI evolves is similar
403 across this clade. The few comparative data on the rate at which RI evolves suggests that it can
404 vary across broad clades (Rabosky and Matute 2013). However, for a clade like this, which
405 consists of broadly related, morphologically and ecologically-similar lizards found in a similar
406 biogeographic context, we suspect there is likely to be less variation. Indeed, RI and divergence
407 time correlate closely across five sister-species comparisons in *Carlia*, *Lampropholis,* and a
408 closely-related genus, *Saproscincus* (Singhal and Moritz 2013; Singhal and Bi 2017). Further, and
409 importantly, these lineages likely resulted from similar speciation processes – *i.e.*, these deep,
410 cryptic lineages evolved due to very long periods of isolation in environmentally similar refugia
411 (see below). Therefore, we believe we can sensibly extrapolate our results across other cryptic
412 congeneric lineages that diverged under similar processes.
413 To extrapolate, we use the divergence between *C. rubrigularis* N and S as our cutoff
414 because they are the youngest lineage-pair for which we have solid evidence of RI. Divergence
415 estimates are highly correlated across the three metrics for genetic divergence ($r \sim 0.7 – 9$; Fig. 3).

Still, we take a conservative approach and only elevate those lineages that show greater divergence than what is seen for *C. rubrigularis* N and S across all metrics (with one exception, below). Notably, this cutoff is greater than that seen among several comparisons between nominal taxa (Fig. 3). Divergences between *L. robertsi* CU and TU, *L. robertsi* BK and BFAU, and *C. rhomboidalis* N and S all fall below this cutoff (Table S5), so we recognize these as phylogeographic lineages within species. However, the divergence between *L. robertsi* BK/BFAU and *L. robertsi* CU/TU is greater than this cutoff. Accordingly, we propose to diagnose the BK/BFAU and CU/TU allopatric lineages as species; this deep divergence suggests they are likely to exhibit RI should they ever come into contact. We use these groupings for morphological comparisons, as well.

The case of *L. coggeri* EU is more ambiguous, when considering genetic data alone. *Lampropholis coggeri* EU is most closely related to *L. coggeri* N/C, and divergence falls just below our proposed cutoff for raw divergence and branching time (Fig. 3A, 3C) but just above the cutoff for net divergence (Fig. 3B). However, *L. coggeri* EU sits isolated off the far south end of the Wet Tropics, geographically closest to *L. coggeri* S. Therefore, it is much more likely to interact with *L. coggeri* S in future, with which it shows much greater divergence (Fig. 1, Fig. 3; Table S5). Further, alone among the comparisons made here, *L. coggeri* EU is morphologically (and perhaps ecologically; see below) distinct from *L. coggeri* S (Table 1). Because the *L. coggeri* S and EU comparison is more salient than the *L. coggeri* C and EU comparison, we further propose to elevate *L. coggeri* EU as a separate species.

The formal taxonomic revisions of these lineages are presented in Appendix 1. To summarize, we revise the '*C. rubrigularis*' group to retain *C. wundalthini* and *C. rhomboidalis*,

retain *C. rubrigularis* S as *C. rubrigularis*, and elevate *C. rubrigularis* N to *C. crypta* **sp. nov**. For the '*L. coggeri*' group, we retain *L. coggeri* N/C as *L. coggeri*, elevate *L. coggeri* S to *L. similis* **sp. nov**., and elevate *L. coggeri* EU to *L. elliotensis* **sp. nov**. For the '*L. robertsi*' group, we retain *L. robertsi* CU/TU as *L. robertsi* and elevate *L. robertsi* BFAU/BK to *L. bellendenkerensis* **sp. nov**.

Speciation processes and cryptic species

Extrapolating a divergence cutoff as done here works, in part, because the Wet Tropics lineages likely share similar divergence histories and processes. These taxa diverged through extended periods of isolation in environmentally-similar, climatically-stable rainforest refugia, resulting in genetic divergence but eco-morphological conservatism (Graham et al. 2006; Moritz et al. 2009). The widespread Wet Tropics lineages (*C. rubrigularis* N and S; *L. coggeri* N/C and S) occupy similar habitats, and the lineages of '*L. robertsi*' occupy mountaintop habitats that appear broadly similar. The morphological stasis in these cryptic species therefore likely reflects a lack of divergent selection across similar environments (Moritz et al. 2009; Hoskin et al. 2011).

Only those lineages peripheral to the main block of the Wet Tropics rainforests exhibit morphological divergence. For example, *L. coggeri* EU differs subtly in body shape from other species in the group; it also occupies a subset of the habitats occupied by the other lineages in the '*L. coggeri*' group. Whereas the other lineages are found across a broad range of rainforest types and habitat edges, *L. coggeri* EU is found only in mesic pockets of rocky, upland rainforest. Greater morphological divergence is seen in the two lineages in the '*C. rubrigularis*' group found outside the Wet Tropics region: *C. wundalthini* and *C. rhomboidalis*. Despite being of similar age as other lineages (Fig. 2), these species are distinct for male breeding coloration and some

aspects of body size and shape. As seen across other Wet Tropics taxa, phenotypic divergence is only recovered in association with environmentally-driven selection – e.g., across ecotones (Schneider and Moritz 1999), in peripheral isolates (Hoskin et al. 2011), or reinforcing selection in hybrid zones (Hoskin et al. 2005). These cryptic species thus underline the importance of "non-ecological" mechanisms in speciation (Schluter 2001), in particular, mutation-order speciation (Mani and Clarke 1990; Nosil and Flaxman 2011).

This work also helps further outline the distinction between historical and current patterns of hybridization and introgression (Edwards et al. 2016). The biological species concept requires current introgression to be limited, but both theoretical models and empirical data show that species can diverge and remain distinct in the presence of historical gene flow (Nosil 2008; Pinho and Hey 2010). Similarly, our tests for introgression suggest there has been introgression between at least four lineage-pairs (Fig. 2), all of which are either previously-recognized or now elevated nominal species. Yet, for at least two of these lineage-pairs (*C. rubrigularis* N and S and *L. coggeri* C and S), our analysis of current patterns shows that hybridization occurs but is geographically highly-restricted (Fig. 4). This distinction between historical and current patterns illustrates the complicated relationship between gene flow and species borders.

The practicality of delimiting cryptic species

Genetic divergences for almost all our lineage comparisons falls in the so-called "gray zone" of speciation, in which lineages transition from behaving as populations to species (Roux et al. 2016). Defined by net silent divergence (d_a) at coding nuclear genes, this gray zone spans

482 divergences from 0.5% to 2%. Given that many cryptic lineages originated during glacial cycles
483 over the last few million years (Hewitt 2000), many of them should fall within this four-fold
484 range of divergence. This underlines the challenge in delimiting cryptic lineages – many of
485 them have a biogeographic and divergence history that places them in an ambiguous zone of
486 divergence, where lineages are as likely to merge or remain distinct upon secondary contact.
487 Given this ambiguity, identifying strong phylogeographic structure within species
488 should be just the first step in diagnosing species boundaries across cryptic boundaries (Fig. 6,
489 Table 2). Additional validation is required, which we loosely group into four categories: (1)
490 statistical species delimitation, (2) post-hoc discovery of phenotypic differences that delimit
491 lineages (*i.e.*, integrative taxonomy; (Padial et al. 2010)), (3) indirect or direct estimates of
492 evolutionary isolation between lineages, or (4) calibration-based approaches. Here, we outline
493 these approaches briefly and explain their conceptual and practical benefits and limitations.
494 Note that after applying any of these approaches, researchers must still formally revise the
495 taxonomy for these validations to be recognized. However, all too often, these taxonomic
496 revisions are not done (Carstens et al. 2013; Pante et al. 2014).
497 First, perhaps the most common approach currently used is statistical species
498 delimitation, which applies coalescent-based methods to determine which lineages are
499 genetically unique (Ence and Carstens 2011; Yang and Rannala 2014). Often, statistical
500 approaches are used as an early step to more quantitatively assess visual clusters, and in other
501 studies, they are used as a final stage of analysis to diagnose species (Fig. 6). Across our three
502 species groups, statistical species delimitation diagnosed all putative lineages as species (Fig. 2).
503 Yet, this statistical diagnosis contrasts to our biological understanding of species boundaries.

504 For example, although *L. coggeri* N and C are statistically distinct, introgression between them is
505 widespread genomically and geographically (Fig. 4). This disconnect reflects the emerging
506 consensus that, although statistical species delimitation methods can robustly identify
507 populations, these populations are not always equivalent to species (Rosenblum et al. 2012;
508 Dynesius and Jansson 2014; Sukumaran and Knowles 2017). In other words, the genetic
509 distinctiveness of a population does not necessarily confer robust evolutionary distinctiveness
510 as envisaged under the Biological Species Concept. Thus, we take a deliberately conservative
511 approach and refrain from elevating morphologically cryptic lineages whose sole support is
512 from statistical analyses of genetic data (Oliver et al. 2015). However, statistical approaches to
513 species delimitation are the most efficient and flexible method across taxonomic groups and are
514 likely to remain an attractive option for many study systems, even if these approaches alone
515 provide insufficient evidence to denote robust taxa.

516 Second, while mostly not true in the present study (Fig. 5), researchers often discover
517 post-hoc phenotypic differences after further investigation of putative cryptic lineages, leading
518 to so-called pseudo-cryptic species (Knowlton 1993). For example, cryptic lineages might vary
519 in traits that facilitate RI between lineages (e.g., mating calls, (Barber 1951)) or ecological co-
520 existence (e.g., divergence in life-history; (Leys et al. 2017)). Often, however, these phenotypic
521 differences might only relate trivially to how distinctive a lineage is – *i.e.*, minor differences in
522 scale counts. In such cases, phenotypic differentiation alone might not necessarily confer
523 evolutionary distinctiveness, and further validation would be required.

524 Third, researchers can assay strength of RI between lineages either through indirect
525 studies of contact zones, observation of sympatry among cryptic lineages, or laboratory- or

field-based tests of mate choice and hybrid fitness (Blair 1972; Hoskin et al. 2005; Dolman 2008). As shown in this work (Fig. 4), these approaches offer detailed data on how likely lineages are to remain distinct if and when they overlap with their congenerics. However, these approaches are often quite practically limited—generating these data can require contiguous ranges, high population densities, organisms amenable to experimentation, and substantial investment in both time and money. These practical limitations surfaced in the present work; we were unable to test for RI between allopatric lineages, nor could we bring them into a laboratory setting. Barring this, alternative approaches could be used to identify cases of abrupt genetic boundaries across dense sampling or test for geographically-extensive introgression across lineage boundaries using large numbers of markers (Melville et al. 2017).

For those lineages not amenable to indirect or direct testing for RI, we used a fourth general approach: using calibrations to determine how much divergence is sufficient to elevate a species. In the DNA barcoding literature, these calibrations are typically informed by patterns of divergence among nominal taxa, although they are used across broad swaths of the tree of life—*i.e.*, all birds or all butterflies (Hebert et al. 2004b; Janzen et al. 2005). Another option is to use calibrations informed by data on the tempo at which RI evolves in closely-related taxa, as done in this study. While this approach still requires the expensive and time-consuming generation of data on isolation between lineages, the cutoff is more principled than barcode gaps. Unlike barcode gaps, which are applied widely across taxonomic groups, our cutoff is based on the observed isolation between lineages within a given clade, which likely share a common mode of lineage divergence and speciation. Such an approach allows us to tackle cryptic diversity while reflecting the variable nature of the speciation process. Moving forward,

548 we will explore whether this cutoff could contribute to diagnosing species boundaries among
549 phylogeographic lineages of other species of *Carlia* (Potter et al. 2016).
550 Across all these approaches, a potential flaw is insufficient sampling of species ranges.
551 In particular, by sampling two ends of an array of populations, we can infer distinction between
552 lineages where gene flow is actually continuous throughout (Pante et al. 2015). Because all
553 approaches to cryptic species validation either have conceptual or practical weaknesses (Table
554 2), the ideal approach will likely vary across taxonomic groups. For example, in the Wet
555 Tropics, phylogeographic studies have recovered deep splits in other taxa outside of lizards,
556 including frogs and mammals (Moritz et al. 2009). For the frog lineages, many of which occur in
557 dense numbers, meet in narrow contact zones, and are amenable to breeding experiments, data
558 on hybridization patterns and mate choice have helped validate putative cryptic lineages and
559 led to the formal revision of lineages (Hoskin et al. 2005; Hoskin 2007). However, for mammals,
560 density is too low to allow indirect or direct tests of isolation, so other approaches will be
561 required.
562 Importantly, the framework we applied here—generating initial descriptions of within-
563 species phylogeographic diversity (Dolman and Moritz 2006; Bell et al. 2010), confirming these
564 patterns with multilocus data sets, and then inferring fine-scale patterns of current RI (Phillips
565 et al. 2004; Singhal and Moritz 2012, 2013; Singhal and Bi 2017)—represents a significant
566 investment in time and money. For many systems, this approach is simply not tenable, and
567 further, often too slow where decisions on species limits have immediate conservation
568 consequences (Hedin 2015). That said, given the dangers of 'taxonomic overinflation' (Isaac et
569 al. 2004; Frankham et al. 2012), we advocate that researchers validate putative cryptic lineages

by both considering statistical delimitation approaches and other data on the biological reality of lineages, whether that be direct or indirect evidence for isolation.

CONCLUSION

Cryptic species challenge traditional notions of species, because the discrepancy between morphological and genetic axes of divergence can make them hard to categorize. Yet, other data suggest that many cryptic species are phenotypically divergent, but on axes of variation that are harder to measure (e.g., mating pheromones in lizards). In cases where we cannot identify phenotypic differences, like the lizards of the Wet Tropics, we can test the validity of these lineages through other means, such as looking at interactions between cryptic lineages in parapatry. Often, these richer, more integrative datasets complement genetic data and show that cryptic lineages are independently evolving units. However, as we also see in these taxa, despite marked genetic differentiation, some cryptic lineages might just be ephemera, destined to be lost to hybridization with congeneric lineages, if they meet in the future. These data remind us that species boundaries are hypotheses (Fujita et al. 2012), our best estimate of the fate of these lineages and a recognition of the ever-evolving nature of species (Darwin 1859; Mallet 1995).

ACKNOWLEDGEMENTS

We thank J. Bragg and also staff at UMich Arc TS Flux for advice and logistical support. In addition, we gratefully acknowledge the members of the C. Moritz & S. Williams research groups, both past and present, who have contributed samples, environmental data, and their

expertise to the Wet Tropics research program. Funding for this project came from a National Science Foundation Post-doctoral Research Fellowship in Biology (NSF #1519732 to SS), grants from the Australian Research Council (ARC), the Australian Biological Resources Study (ABRS) and the National Science Foundation to CM, and grants from the ARC and ABRS to CH.

DATA ACCESSIBILITY

- Raw sequencing data: to be deposited in NCBI SRA upon acceptance
- Pseudo-reference files and variant sets: DataDryad accession 10.5061/dryad.g7v1b
- Code used to generate data: https://github.com/singhal/AWT_delimit and https://github.com/singhal/SqCL
- Specimens used for morphological analyses & species descriptions: all are deposited at Queensland Museum for research use; accession numbers available in Appendix 1.

614 **TABLES**

615 Table 1. Testing for morphological differences in body size and shape between the major
616 lineages in each species group. Body size was tested using nested ANOVA. Body shape was
617 tested using nested MANOVA ('lineage' overall effect and planned contrasts), and using Wilks'
618 Lambda as the F-statistic.

619 Table 2: A survey of approaches that can be used to validate putative cryptic lineages and the
620 benefits and limitations of each approach. We highlight which approaches were used in the
621 present study and identify other examples from the broader literature; this list of examples is
622 meant to be illustrative not exhaustive. Many of the studies that validated putative cryptic
623 species did not also conduct a formal taxonomic revision.

FIGURES

Figure 1: Geographic distribution of lineages in the three groups; boundaries were inferred after sequencing an average of 27 individuals for mtDNA and 12 for nDNA (Table S1; Fig. S2). Points represent localities for samples included in this study. (A) The five lineages in the '*Carlia rubrigularis*' group: *C. wundalthini*, *C. rubrigularis* N, *C. rubrigularis* S, *C. rhomboidalis* N, and *C. rhomboidalis* S, (B) the four lineages in the '*Lampropholis coggeri*' group: *L. coggeri* N, *L. coggeri* C, *L. coggeri* S, and *L. coggeri* EU, and (C) the four lineages in the '*L. robertsi*' group: *L. robertsi* CU, *L. robertsi* BFAU, *L. robertsi* TU, *L. robertsi* BK. In the inset map, the distribution of the rainforest is shown in light green. Like many phylogeographic lineages, these lineages are geographically circumscribed, and their ranges either are geographically proximate or narrowly overlapping. Pictures courtesy of B. Phillips, C. Peng, and S. Zozaya (L-R).

Figure 2: Species tree for the included taxa as inferred using STARBEAST2 with 200 randomly selected exons. This topology and branching times are robust across multiple random samples (Fig. S2). Nodes with ≥95% local posterior probability are indicated with filled circles. Nodes for which BPP inferred ≥95% probability of a speciation event are shown by open circles. STACEY results match BPP results and are not shown. Arrows indicate pairwise relationships for which there is significant evidence for historical introgression (Table S6). The phylogeographic lineages included in this study all diverged over a relatively narrow span of time.

Figure 3: Patterns of divergence between pairwise lineage-comparisons for (A) d_{xy} for silent sites in mitochondrial DNA (mtDNA) and nuclear DNA (nDNA), (B) d_a at silent sites in mtDNA and

nDNA, and (C) branching times in units of substitutions per site per million years and d_a at mtDNA; branching times were inferred from the tree depicted in Fig. 1. Each pairwise comparison is coded as either being between (1) recognized: two lineages that were already recognized at the species-level, (2) elevated: two lineages that were elevated in the current study, or (3) population: lineages for which there is insufficient evidence to elevate them to species. Arrows identify the three pairwise comparisons for which we have data on reproductive isolation from contact zone studies (Fig. 4), the gray line indicates the transition point at which we first recover evidence for isolation between lineages (*i.e.*, between *Carlia rubrigularis* N and S). Many of the lineages that we propose to elevate are more diverged than nominal species.

Figure 4: Evidence for rates of hybridization and introgression at three contact zones between lineages included in this analysis: *Carlia rubrigularis* N and S, *Lampropholis coggeri* C and S, and *L. coggeri* N and C. Contacts are listed in the legend in order of least to most divergent. (A) Percent of individuals in the center of contact zones that were identified as hybrid. A hybrid individual was defined as individuals that had ≥10% membership in both parental species as determined by STRUCTURE. (B) Distribution of cline widths in the contact zone across an average of 9.5K clines. (C) The extent of linkage disequilibrium in each contact zone. Moran's I measures the autocorrelation in cline widths across the genome, which serves as a proxy for linkage disequilibrium. These genetic estimates of reproductive isolation show evidence for selection against hybrids in *C. rubrigularis* N and S and *L. coggeri* C and S.

Figure 5: Scatter plots of PC1 (representing body size) and PC2 (the primary axis of body shape) in each of the species groups: (A) '*Carlia rubrigularis*' group, (B) '*Lampropholis coggeri*' group, (C) '*Lampropholis robertsi*' group. See Tables S7 – 9 for details on loadings of PC2. Morphological divergence among the lineages in each species group is limited, with the exception of some shape divergence in *L. coggeri* EU.

Figure 6: A flowchart outlining a possible research approach to validating cryptic lineages. Statistical species delimitation is often used to both define putative lineages and to validate them. Width and contrast of validation arrows indicate how robust we believe these approaches are. Benefits and limitations of each approach are further described in Table 2.

REFERENCES

Adams, M., T. A. Raadik, C. P. Burridge, and A. Georges. 2014. Global biodiversity assessment and hyper-cryptic species complexes: more than one species of elephant in the room? Systematic Biology 63:518-533.

Amato, A., W. H. Kooistra, J. H. L. Ghiron, D. G. Mann, T. Pröschold, and M. Montresor. 2007. Reproductive isolation among sympatric cryptic species in marine diatoms. Protist 158:193-207.

Bálint, M., S. Domisch, C. Engelhardt, P. Haase, S. Lehrian, J. Sauer, K. Theissinger, S. Pauls, and C. Nowak. 2011. Cryptic biodiversity loss linked to global climate change. Nature Climate Change 1:313-318.

Barber, H. S. 1951. North American fireflies of the genus Photuris. Smithsonian Institution.

Barton, N. 1983. Multilocus clines. Evolution 37:454-471.

Barton, N. H. and K. S. Gale. 1993. Genetic analysis of hybrid zones. Hybrid zones and the evolutionary process:13-45.

Bell, R. C., J. L. Parra, M. Tonione, C. J. Hoskin, J. B. Mackenzie, S. E. Williams, and C. Moritz. 2010. Patterns of persistence and isolation indicate resilience to climate change in montane rainforest lizards. Molecular Ecology 19:2531-2544.

Bickford, D., D. J. Lohman, N. S. Sodhi, P. K. Ng, R. Meier, K. Winker, K. K. Ingram, and I. Das. 2007. Cryptic species as a window on diversity and conservation. Trends in Ecology & Evolution 22:148-155.

Blair, W. F. 1972. Evolution in the genus Bufo. University of Texas Press, Austin, Texas.

Bolger, A. M., M. Lohse, and B. Usadel. 2014. Trimmomatic: a flexible trimmer for Illumina sequence data. Bioinformatics 30:2114-2120.

Bolnick, D. I., T. J. Near, and P. C. Wainwright. 2006. Body size divergence promotes post-zygotic reproductive isolation in centrarchids. Evolutionary Ecology Research 8:903-913.

Bragg, J. G., S. Potter, A. C. Afonso Silva, C. J. Hoskin, B. Y. H. Bai, and C. Moritz. 2018. Phylogenomics of a rapid radiation: the Australian rainbow skinks. BMC Evolutionary Biology 18:15.

Bragg, J. G., S. Potter, K. Bi, and C. Moritz. 2016. Exon capture phylogenomics: efficacy across scales of divergence. Molecular Ecology Resources 16:1059-1068.

Brown, J. M., S. M. Hedtke, A. R. Lemmon, and E. M. Lemmon. 2009. When trees grow too long: investigating the causes of highly inaccurate Bayesian branch-length estimates. Systematic Biology 59:145-161.

Carstens, B. C., T. A. Pelletier, N. M. Reid, and J. D. Satler. 2013. How to fail at species delimitation. Molecular Ecology 22:4369-4383.

Carstens, B. C. and J. D. Satler. 2013. The carnivorous plant described as *Sarracenia alata* contains two cryptic species. Biological Journal of the Linnean Society 109:737-746.

Coyne, J. A. and H. A. Orr. 1989. Patterns of speciation in Drosophila. Evolution 43:362-381.

Darwin, C. 1859. The origin of species by means of natural selection: or, the preservation of favored races in the struggle for life. John Murray, London, UK.

de León, G. P.-P. and R. Poulin. 2016. Taxonomic distribution of cryptic diversity among metazoans: not so homogeneous after all. Biology Letters 12:20160371.

De Queiroz, K. 2007. Species concepts and species delimitation. Systematic Biology 56:879-886.
Dolman, G. 2008. Evidence for differential assortative female preference in association with refugial isolation of rainbow skinks in Australia's tropical rainforests. PLoS One 3:e3499.
Dolman, G. and C. Moritz. 2006. A multilocus perspective on refugial isolation and divergence in rainforest skinks (*Carlia*). Evolution 60:573-582.
Durand, E. Y., N. Patterson, D. Reich, and M. Slatkin. 2011. Testing for ancient admixture between closely related populations. Molecular Biology and Evolution 28:2239-2252.
Dynesius, M. and R. Jansson. 2014. Persistence of within‐species lineages: a neglected control of speciation rates. Evolution 68:923-934.
Eaton, D. A. and R. H. Ree. 2013. Inferring phylogeny and introgression using RADseq data: an example from flowering plants (*Pedicularis*: Orobanchaceae). Systematic Biology 62:689-706.
Edwards, S. V., S. Potter, C. J. Schmitt, J. G. Bragg, and C. Moritz. 2016. Reticulation, divergence, and the phylogeography–phylogenetics continuum. Proceedings of the National Academy of Sciences 113:8025-8032.
Ence, D. D. and B. C. Carstens. 2011. SpedeSTEM: a rapid and accurate method for species delimitation. Molecular Ecology Resources 11:473-480.
Fitzpatrick, B. M. 2002. Molecular correlates of reproductive isolation. Evolution 56:191-198.
Fouquet, A., A. Gilles, M. Vences, C. Marty, M. Blanc, and N. J. Gemmell. 2007. Underestimation of species richness in Neotropical frogs revealed by mtDNA analyses. PLoS One 2:e1109.
Frankham, R., J. D. Ballou, M. R. Dudash, M. D. Eldridge, C. B. Fenster, R. C. Lacy, J. R. Mendelson, I. J. Porton, K. Ralls, and O. A. Ryder. 2012. Implications of different species concepts for conserving biodiversity. Biological Conservation 153:25-31.
Fregin, S., M. Haase, U. Olsson, and P. Alström. 2012. Pitfalls in comparisons of genetic distances: a case study of the avian family Acrocephalidae. Molecular Phylogenetics and Evolution 62:319-328.
Fujita, M. K., A. D. Leaché, F. T. Burbrink, J. A. McGuire, and C. Moritz. 2012. Coalescent-based species delimitation in an integrative taxonomy. Trends in Ecology & Evolution 27:480-488.
Funk, D. J., P. Nosil, and W. J. Etges. 2006. Ecological divergence exhibits consistently positive associations with reproductive isolation across disparate taxa. Proceedings of the National academy of Sciences 103:3209-3213.
Gómez, A., M. Serra, G. R. Carvalho, and D. H. Lunt. 2002. Speciation in ancient cryptic species complexes: evidence from the molecular phylogeny of *Brachionus plicatilis* (Rotifera). Evolution 56:1431-1444.
Gomez, A., P. J. Wright, D. H. Lunt, J. M. Cancino, G. R. Carvalho, and R. N. Hughes. 2007. Mating trials validate the use of DNA barcoding to reveal cryptic speciation of a marine bryozoan taxon. Proceedings of the Royal Society of London B: Biological Sciences 274:199-207.
Grabherr, M. G., B. J. Haas, M. Yassour, J. Z. Levin, D. A. Thompson, I. Amit, X. Adiconis, L. Fan, R. Raychowdhury, and Q. Zeng. 2011. Full-length transcriptome assembly from RNA-Seq data without a reference genome. Nature Biotechnology 29:644-652.

Graham, C. H., C. Moritz, and S. E. Williams. 2006. Habitat history improves prediction of biodiversity in rainforest fauna. Proceedings of the National Academy of Sciences 103:632-636.

Greer, A. 1997. A new species of *Lampropholis* (Squamata: Scincidae) with a restricted, high altitude distribution in eastern Australia. Australian Zoologist 30:360-368.

Hebert, P. D., E. H. Penton, J. M. Burns, D. H. Janzen, and W. Hallwachs. 2004a. Ten species in one: DNA barcoding reveals cryptic species in the neotropical skipper butterfly *Astraptes fulgerator*. Proceedings of the National Academy of Sciences 101:14812-14817.

Hebert, P. D., M. Y. Stoeckle, T. S. Zemlak, and C. M. Francis. 2004b. Identification of birds through DNA barcodes. PLoS Biology 2:e312.

Hedgecock, D. and F. J. Ayala. 1974. Evolutionary divergence in the genus *Taricha* (Salamandridae). Copeia:738-747.

Hedin, M. 2015. High‐stakes species delimitation in eyeless cave spiders (*Cicurina*, Dictynidae, Araneae) from central Texas. Molecular ecology 24:346-361.

Hewitt, G. 2000. The genetic legacy of the Quaternary ice ages. Nature 405:907-913.

Hoskin, C. J. 2007. Description, biology and conservation of a new species of Australian tree frog (Amphibia: Anura: Hylidae: *Litoria*) and an assessment of the remaining populations of *Litoria genimaculata* Horst, 1883: systematic and conservation implications of an unusual speciation event. Biological Journal of the Linnean Society 91:549-563.

Hoskin, C. J. 2014. A new skink (Scincidae: *Carlia*) from the rainforest uplands of Cape Melville, north-east Australia. Zootaxa 3869:224-236.

Hoskin, C. J., M. Higgie, K. R. McDonald, and C. Moritz. 2005. Reinforcement drives rapid allopatric speciation. Nature 437:1353-1356.

Hoskin, C. J., M. Tonione, M. Higgie, J. B. MacKenzie, S. E. Williams, J. VanDerWal, and C. Moritz. 2011. Persistence in peripheral refugia promotes phenotypic divergence and speciation in a rainforest frog. American Naturalist 178:561-578.

Hotaling, S., M. E. Foley, N. M. Lawrence, J. Bocanegra, M. B. Blanco, R. Rasoloarison, P. M. Kappeler, M. A. Barrett, A. D. Yoder, and D. W. Weisrock. 2016. Species discovery and validation in a cryptic radiation of endangered primates: coalescent‐based species delimitation in Madagascar's mouse lemurs. Molecular Ecology 25:2029-2045.

Ingram, G. 1991. Five new skinks from Queensland rainforests. Mem Queensland Mus 30:443-453.

Ingram, G. and J. Covacevich. 1989. Revision of the genus *Carlia* (Reptilia, Scincidae) in Australia with comments on *Carlia bicarinata* of New Guinea. Memoirs of the Queensland Museum 27:443-490.

Isaac, N. J., J. Mallet, and G. M. Mace. 2004. Taxonomic inflation: its influence on macroecology and conservation. Trends in Ecology & Evolution 19:464-469.

Janzen, D. H., M. Hajibabaei, J. M. Burns, W. Hallwachs, E. Remigio, and P. D. Hebert. 2005. Wedding biodiversity inventory of a large and complex Lepidoptera fauna with DNA barcoding. Philosophical Transactions of the Royal Society of London B: Biological Sciences 360:1835-1845.

Jolliffe, I. T. 2002. Principal Component Analysis. Springer-Verlag, New York, NY.

Jones, G. 2017. Algorithmic improvements to species delimitation and phylogeny estimation under the multispecies coalescent. Journal of Mathematical Biology 74:447-467.

Katoh, K., K. Misawa, K. i. Kuma, and T. Miyata. 2002. MAFFT: a novel method for rapid multiple sequence alignment based on fast Fourier transform. Nucleic Acids Research 30:3059-3066.

Kent, W. J. 2002. BLAT—the BLAST-like alignment tool. Genome Research 12:656-664.

King, R. A., A. L. Tibble, and W. O. Symondson. 2008. Opening a can of worms: unprecedented sympatric cryptic diversity within British lumbricid earthworms. Molecular Ecology 17:4684-4698.

Knowlton, N. 1993. Sibling species in the sea. Annual Review of Ecology, Evolution, and Systematics 24:189-216.

Ladner, J. T. and S. R. Palumbi. 2012. Extensive sympatry, cryptic diversity and introgression throughout the geographic distribution of two coral species complexes. Molecular Ecology 21:2224-2238.

Lanfear, R., P. B. Frandsen, A. M. Wright, T. Senfeld, and B. Calcott. 2016. PartitionFinder 2: new methods for selecting partitioned models of evolution for molecular and morphological phylogenetic analyses. Molecular Biology and Evolution 34:772-773.

Leaché, A. D. and M. K. Fujita. 2010. Bayesian species delimitation in West African forest geckos (*Hemidactylus fasciatus*). Proceedings of the Royal Society of London B: Biological Sciences:rspb20100662.

Leys, M., I. Keller, C. T. Robinson, and K. Räsänen. 2017. Cryptic lineages of a common alpine mayfly show strong life‐history divergence. Molecular Ecology 26:1670-1686.

Li, H. and R. Durbin. 2009. Fast and accurate short read alignment with Burrows–Wheeler transform. Bioinformatics 25:1754-1760.

Losos, J. B. 2011. Lizards in an evolutionary tree: ecology and adaptive radiation of anoles. Univ of California Press, Berkeley, CA.

Mallet, J. 1995. A species definition for the modern synthesis. Trends in Ecology & Evolution 10:294-299.

Mani, G. and B. Clarke. 1990. Mutational order: a major stochastic process in evolution. Proceedings of the Royal Society of London B: Biological Sciences 240:29-37.

Mayr, E. 1942. Systematics and the origin of species, from the viewpoint of a zoologist. Harvard University Press, Cambridge, MA.

McDaniel, S. F. and A. J. Shaw. 2003. Phylogeographic structure and cryptic speciation in the trans-Antarctic moss *Pyrrhobryum mnioides*. Evolution 57:205-215.

McKenna, A., M. Hanna, E. Banks, A. Sivachenko, K. Cibulskis, A. Kernytsky, K. Garimella, D. Altshuler, S. Gabriel, and M. Daly. 2010. The Genome Analysis Toolkit: a MapReduce framework for analyzing next-generation DNA sequencing data. Genome Research 20:1297-1303.

Melville, J., M. L. Haines, K. Boysen, L. Hodkinson, A. Kilian, K. L. S. Date, D. A. Potvin, and K. M. Parris. 2017. Identifying hybridization and admixture using SNPs: application of the DArTseq platform in phylogeographic research on vertebrates. Royal Society Open Science 4:161061.

Meyer, M. and M. Kircher. 2010. Illumina sequencing library preparation for highly multiplexed target capture and sequencing. Cold Spring Harbor Protocols 2010:pdb. prot5448.

Moritz, C. and C. Cicero. 2004. DNA barcoding: promise and pitfalls. PLoS Biology 2:e354.

Moritz, C., C. Hoskin, J. B. MacKenzie, B. Phillips, M. Tonione, N. Silva, J. VanDerWal, S. E. Williams, and C. Graham. 2009. Identification and dynamics of a cryptic suture zone in tropical rainforest. Proceedings of the Royal Society of London B: Biological Sciences:rspb. 2008.1622.

Nater, A., M. P. Mattle-Greminger, A. Nurcahyo, M. G. Nowak, M. de Manuel, T. Desai, C. Groves, M. Pybus, T. B. Sonay, and C. Roos. 2017. Morphometric, behavioral, and genomic evidence for a new Orangutan species. Current Biology 27:3487-3498. e3410.

Nei, M. and W.-H. Li. 1979. Mathematical model for studying genetic variation in terms of restriction endonucleases. Proceedings of the National Academy of Sciences 76:5269-5273.

Niemiller, M. L., T. J. Near, and B. M. Fitzpatrick. 2012. Delimiting species using multilocus data: diagnosing cryptic diversity in the southern cavefish, *Typhlichthys subterraneus* (Teleostei: Amblyopsidae). Evolution 66:846-866.

Nosil, P. 2008. Speciation with gene flow could be common. Molecular Ecology 17:2103-2106.

Nosil, P. and S. M. Flaxman. 2011. Conditions for mutation-order speciation. Proceedings of the Royal Society of London B: Biological Sciences 278:399-407.

Ogilvie, H. A., R. R. Bouckaert, and A. J. Drummond. 2017. StarBEAST2 brings faster species tree inference and accurate estimates of substitution rates. Molecular Biology and Evolution:msx126.

Olave, M., E. Solà, and L. L. Knowles. 2014. Upstream analyses create problems with DNA-based species delimitation. Systematic Biology 63:263-271.

Oliver, P., J. S. Keogh, and C. Moritz. 2015. New approaches to cataloguing and understanding evolutionary diversity: a perspective from Australian herpetology. Australian Journal of Zoology 62:417-430.

Oliver, P. M., M. Adams, and P. Doughty. 2010. Molecular evidence for ten species and Oligo-Miocene vicariance within a nominal Australian gecko species (*Crenadactylus ocellatus*, Diplodactylidae). BMC Evolutionary Biology 10:386.

Olsson, U., P. Alström, P. G. Ericson, and P. Sundberg. 2005. Non-monophyletic taxa and cryptic species—evidence from a molecular phylogeny of leaf-warblers (*Phylloscopus*, Aves). Molecular Phylogenetics and Evolution 36:261-276.

Padial, J. M., A. Miralles, I. De la Riva, and M. Vences. 2010. The integrative future of taxonomy. Frontiers in Zoology 7:16.

Pante, E., N. Puillandre, A. Viricel, S. Arnaud‐Haond, D. Aurelle, M. Castelin, A. Chenuil, C. Destombe, D. Forcioli, and M. Valero. 2015. Species are hypotheses: avoid connectivity assessments based on pillars of sand. Molecular Ecology 24:525-544.

Pante, E., C. Schoelinck, and N. Puillandre. 2014. From integrative taxonomy to species description: one step beyond. Systematic Biology 64:152-160.

Pease, J. B. and M. W. Hahn. 2015. Detection and polarization of introgression in a five-taxon phylogeny. Systematic Biology 64:651-662.

Perkins, S. L. 2000. Species concepts and malaria parasites: detecting a cryptic species of *Plasmodium*. Proceedings of the Royal Society of London B: Biological Sciences 267:2345-2350.

Phillips, B. L., S. J. Baird, and C. Moritz. 2004. When vicars meet: a narrow contact zone between morphologically cryptic phylogeographic lineages of the rainforest skink, *Carlia rubrigularis*. Evolution 58:1536-1548.

Pinho, C. and J. Hey. 2010. Divergence with gene flow: models and data. Annual Review of Ecology, Evolution, and Systematics 41:215-230.

Potter, S., J. G. Bragg, B. M. Peter, K. Bi, and C. Moritz. 2016. Phylogenomics at the tips: inferring lineages and their demographic history in a tropical lizard, *Carlia amax*. Molecular Ecology 25:1367-1380.

Rabosky, D. L. and D. R. Matute. 2013. Macroevolutionary speciation rates are decoupled from the evolution of intrinsic reproductive isolation in *Drosophila* and birds. Proceedings of the National Academy of Sciences 110:15354-15359.

Rannala, B. 2015. The art and science of species delimitation. Current Zoology 61:846-853.

Richardson, B. J., P. R. Baverstock, and M. Adams. 1986. Allozyme electrophoresis: a handbook for animal systematics and population studies. Academic Press, San Diego, California.

Rissler, L. J. and J. J. Apodaca. 2007. Adding more ecology into species delimitation: ecological niche models and phylogeography help define cryptic species in the black salamander (*Aneides flavipunctatus*). Systematic Biology 56:924-942.

Ronquist, F., M. Teslenko, P. Van Der Mark, D. L. Ayres, A. Darling, S. Höhna, B. Larget, L. Liu, M. A. Suchard, and J. P. Huelsenbeck. 2012. MrBayes 3.2: efficient Bayesian phylogenetic inference and model choice across a large model space. Systematic Biology 61:539-542.

Rosenblum, E. B., B. A. Sarver, J. W. Brown, S. Des Roches, K. M. Hardwick, T. D. Hether, J. M. Eastman, M. W. Pennell, and L. J. Harmon. 2012. Goldilocks meets Santa Rosalia: an ephemeral speciation model explains patterns of diversification across time scales. Journal of Evolutionary Biology 39:255-261.

Rosindell, J., S. J. Cornell, S. P. Hubbell, and R. S. Etienne. 2010. Protracted speciation revitalizes the neutral theory of biodiversity. Ecology Letters 13:716-727.

Roux, C., C. Fraisse, J. Romiguier, Y. Anciaux, N. Galtier, and N. Bierne. 2016. Shedding light on the grey zone of speciation along a continuum of genomic divergence. PLoS Biology 14:e2000234.

Sasa, M. M., P. T. Chippindale, and N. A. Johnson. 1998. Patterns of postzygotic isolation in frogs. Evolution 52:1811-1820.

Schluter, D. 2001. Ecology and the origin of species. Trends in Ecology & Evolution 16:372-380.

Schneider, C. and C. Moritz. 1999. Rainforest refugia and Australia's Wet Tropics. Proceedings of the Royal Society of London B: Biological Sciences 266:191-196.

Schonrogge, K., B. Barr, J. C. Wardlaw, E. Napper, M. G. Gardner, J. Breen, G. W. Elmes, and J. A. Thomas. 2002. When rare species become endangered: cryptic speciation in myrmecophilous hoverflies. Biological Journal of the Linnean Society 75:291-300.

Seehausen, O., G. Takimoto, D. Roy, and J. Jokela. 2008. Speciation reversal and biodiversity dynamics with hybridization in changing environments. Molecular Ecology 17:30-44.

Silva, A. C. A., N. Santos, H. A. Ogilvie, and C. Moritz. 2017. Validation and description of two new north-western Australian Rainbow skinks with multispecies coalescent methods and morphology. PeerJ 5:e3724.

Singhal, S. 2013. De novo transcriptomic analyses for non‐model organisms: an evaluation of methods across a multi‐species data set. Molecular Ecology Resources 13:403-416.

Singhal, S. and K. Bi. 2017. History cleans up messes: the impact of time in driving divergence and introgression in a tropical suture zone. Evolution 71:1888-1899.

Singhal, S. and C. Moritz. 2012. Strong selection against hybrids maintains a narrow contact zone between morphologically cryptic lineages in a rainforest lizard. Evolution 66:1474-1489.

Singhal, S. and C. Moritz. 2013. Reproductive isolation between phylogeographic lineages scales with divergence. Proceedings of the Royal Society of London B: Biological Sciences 280:20132246.

Sites, J. W., N. H. Barton, and K. M. Reed. 1995. The genetic structure of a hybrid zone between two chromosome races of the *Sceloporus grammicus* complex (Sauria, Phrynosomatidae) in Central Mexico. Evolution:9-36.

Skinner, A., A. F. Hugall, and M. N. Hutchinson. 2011. Lygosomine phylogeny and the origins of Australian scincid lizards. Journal of Biogeography 38:1044-1058.

Slater, G. S. C. and E. Birney. 2005. Automated generation of heuristics for biological sequence comparison. BMC Bioinformatics 6:31.

Smith, M. A., J. J. Rodriguez, J. B. Whitfield, A. R. Deans, D. H. Janzen, W. Hallwachs, and P. D. Hebert. 2008. Extreme diversity of tropical parasitoid wasps exposed by iterative integration of natural history, DNA barcoding, morphology, and collections. Proceedings of the National Academy of Sciences 105:12359-12364.

Smith, M. A., N. E. Woodley, D. H. Janzen, W. Hallwachs, and P. D. Hebert. 2006. DNA barcodes reveal cryptic host-specificity within the presumed polyphagous members of a genus of parasitoid flies (Diptera: Tachinidae). Proceedings of the National Academy of Sciences of the United States of America 103:3657-3662.

Stewart, K. A. and S. C. Lougheed. 2013. Testing for intraspecific postzygotic isolation between cryptic lineages of *Pseudacris crucifer*. Ecology and Evolution 3:4621-4630.

Struck, T. H., J. L. Feder, M. Bendiksby, S. Birkeland, J. Cerca, V. I. Gusarov, S. Kistenich, K.-H. Larsson, L. H. Liow, and M. D. Nowak. in press. Finding Evolutionary Processes Hidden in Cryptic Species. Trends in Ecology & Evolution.

Stuart, B. L., R. F. Inger, and H. K. Voris. 2006. High level of cryptic species diversity revealed by sympatric lineages of Southeast Asian forest frogs. Biology Letters 2:470-474.

Suatoni, E., S. Vicario, S. Rice, T. Snell, and A. Caccone. 2006. An analysis of species boundaries and biogeographic patterns in a cryptic species complex: the rotifer—*Brachionus plicatilis*. Molecular Phylogenetics and Evolution 41:86-98.

Sukumaran, J. and L. L. Knowles. 2017. Multispecies coalescent delimits structure, not species. Proceedings of the National Academy of Sciences 114:1607-1612.

Sunnucks, P. and D. F. Hales. 1996. Numerous transposed sequences of mitochondrial cytochrome oxidase I-II in aphids of the genus *Sitobion* (Hemiptera: Aphididae). Molecular Biology and Evolution 13:510-524.

Tellier, F., J. A. Vega, B. R. Broitman, J. A. Vasquez, M. Valero, and S. Faugeron. 2011. The importance of having two species instead of one in kelp management: the *Lessonia nigrescens* species complex. Cah. Biol. Mar:52.

Turner, J. R. 1967. Why does the genotype not congeal? Evolution 21:645-656.

Vilas, R., C. Criscione, and M. Blouin. 2005. A comparison between mitochondrial DNA and the ribosomal internal transcribed regions in prospecting for cryptic species of platyhelminth parasites. Parasitology 131:839-846.

Winger, B. M. and J. M. Bates. 2015. The tempo of trait divergence in geographic isolation: avian speciation across the Marañon Valley of Peru. Evolution 69:772-787.

Witt, J. D., D. L. Threloff, and P. D. Hebert. 2006. DNA barcoding reveals extraordinary cryptic diversity in an amphipod genus: implications for desert spring conservation. Molecular Ecology 15:3073-3082.

Yang, Z. and B. Rannala. 2014. Unguided species delimitation using DNA sequence data from multiple loci. Molecular Biology and Evolution 31:3125-3135.

Zhang, C., D.-X. Zhang, T. Zhu, and Z. Yang. 2011. Evaluation of a Bayesian coalescent method of species delimitation. Systematic Biology 60:747-761.

Zhang, J., K. Kobert, T. Flouri, and A. Stamatakis. 2013. PEAR: a fast and accurate Illumina Paired-End reAd mergeR. Bioinformatics 30:614-620.

Table 1. Testing for morphological differences in body size and shape between the major lineages in each species group. Body size was tested using nested ANOVA. Body shape was tested using nested MANOVA ('lineage' overall effect and planned contrasts), and using Wilks' Lambda as the F-statistic.

	F	d.f., numerator	d.f., denominator	p-value	Sig.
'*C. rubrigularis*' N vs S					
Body size (PC1)	1.17	1	50	0.29	
Body shape (PC2 - PC5)	0.45	4	5	0.77	
'*L. robertsi*' CU/TU vs BK/BFAU					
Body size (PC1)	3.89	1	28	0.06	
Body shape (PC2 - PC5)	2.68	3	1	0.42	
'*L. coggeri*' N/C vs S vs EU					
Body size (PC1)	2.46	2	58	0.09	
Body shape (PC2 - PC5)	3.46	8	10	0.04	*
multivariate contrasts N/C vs. S	2.56	4	5	0.17	
N/C vs. EU	3.35	4	5	0.11	
S vs. EU	5.00	4	5	0.05	*

Table 2: A survey of approaches that can be used to validate putative cryptic lineages and the benefits and limitations of each approach. We highlight which approaches were used in the present study and identify other examples from the broader literature; this list of examples is meant to be illustrative not exhaustive. Many of the studies that validated putative cryptic species did not also conduct a formal taxonomic revision.

Approaches to validate putative cryptic species	**Benefits**	**Limitations**	**Examples from this study**	**Other examples**
Statistical species delimitation	efficient and affordable; can be applied to asexual and sexual organisms; many methods can handle ancestral polymorphism	populations cannot be easily distinguished from true species (Sukumaran and Knowles 2017); different approaches often lead to differing results (Carstens et al. 2013); results can be deceiving in the presence of gene-flow		geckos (Leaché and Fujita 2010),carnivorous plants (Carstens and Satler 2013), cavefish (Niemiller et al. 2012), mouse lemurs (Hotaling et al. 2016)
Identification of morphological, behavioral, physiological differences among 'pseudo' cryptic lineages	can lead to the identification of divergence in traits that are likely to keep lineages distinct (e.g., ecological differences, phenological shifts, mating calls)	phenotypic differences do not guarantee that lineages will remain distinct if they interact (e.g., ((Hoskin et al. 2005))	*L. coggeri* EU	lizards (Silva et al. 2017), hoverflies (Schonrogge et al. 2002), mayflies (Leys et al. 2017), wasps (Smith et al. 2008), butterflies (Hebert et al. 2004a), salamanders (Rissler and Apodaca 2007), frogs (Hoskin et al. 2011)
Identification of range overlap among cryptic species	offers robust evidence that lineages are not interbreeding	many cryptic species are parapatric or allopatric, so not applicable to many taxa		rotifers (Gómez et al. 2002), frogs (Stuart et al. 2006), *Plasmodium* (Perkins 2000), earthworms (King et al. 2008), fish (Adams et al. 2014)

Direct estimates of reproductive isolation through mate choice studies and crossing experiments	offers robust evidence that lineages are not interbreeding	can only be used for sexually reproducing species that are amenable to lab husbandry; expensive and time-consuming; lab-based estimates of mate choice and hybrid fitness can differ from field-based estimates		rotifers (Suatoni et al. 2006), bryozoans (Gomez et al. 2007), diatoms (Amato et al. 2007), frogs (Hoskin et al. 2005)
Indirect estimates of reproductive isolation from regions of parapatry or sympatry	allows indirect measure of factors structuring extent of gene flow between lineages such as extent of assortative mating, genetic incompatibilities, etc.	can only be used for sexually reproducing species that co-occur and exist at sufficient density for sampling; indirect estimates can be influenced by often uncharacterized demographic factors	*C. rubrigularis* N, *C. rubrigularis* S, *L. coggeri* C, *L. coggeri* S	frogs (Stewart and Lougheed 2013), lizards (Sites et al. 1995), kelp (Tellier et al. 2011), corals (Ladner and Palumbi 2012)
Using calibrations of RI vs. genomic divergence based on data from closely-related species	provides a well-informed guideline for species that are likely to evolve reproductive isolation at a similar tempo	still requires the extensive and expensive collection of data on reproductive isolation in closely-related species	*L. robertsi* TU/CU, *L. robertsi* BK/ BFAU	
Using calibrations based on sequence divergence	efficient and affordable; can be applied to asexual and sexual organisms; can be more clade-specific if informed by patterns of divergence between nominal species in the clade	not conceptually well-grounded (but see (Roux et al. 2016)); what metric of divergence to use is unclear (Fregin et al. 2012), clades might vary in the rate at which they evolve reproductive barriers (Rabosky and Matute 2013)		caddisflies (Bálint et al. 2011), platyhelminth (Vilas et al. 2005), frogs (Fouquet et al. 2007), amphipods (Witt et al. 2006), birds (Olsson et al. 2005), parasitoid flies (Smith et al. 2006)

A

C. wundalthini
C. rubrigularis N
C. rubrigularis S
C. rhomboidalis N
C. rhomboidalis S

B

L. coggeri N
L. coggeri C
L. coggeri S
L. coggeri EU

C

L. robertsi TU
L. robertsi CU
L. robertsi BK
L. robertsi BFAU

100 km

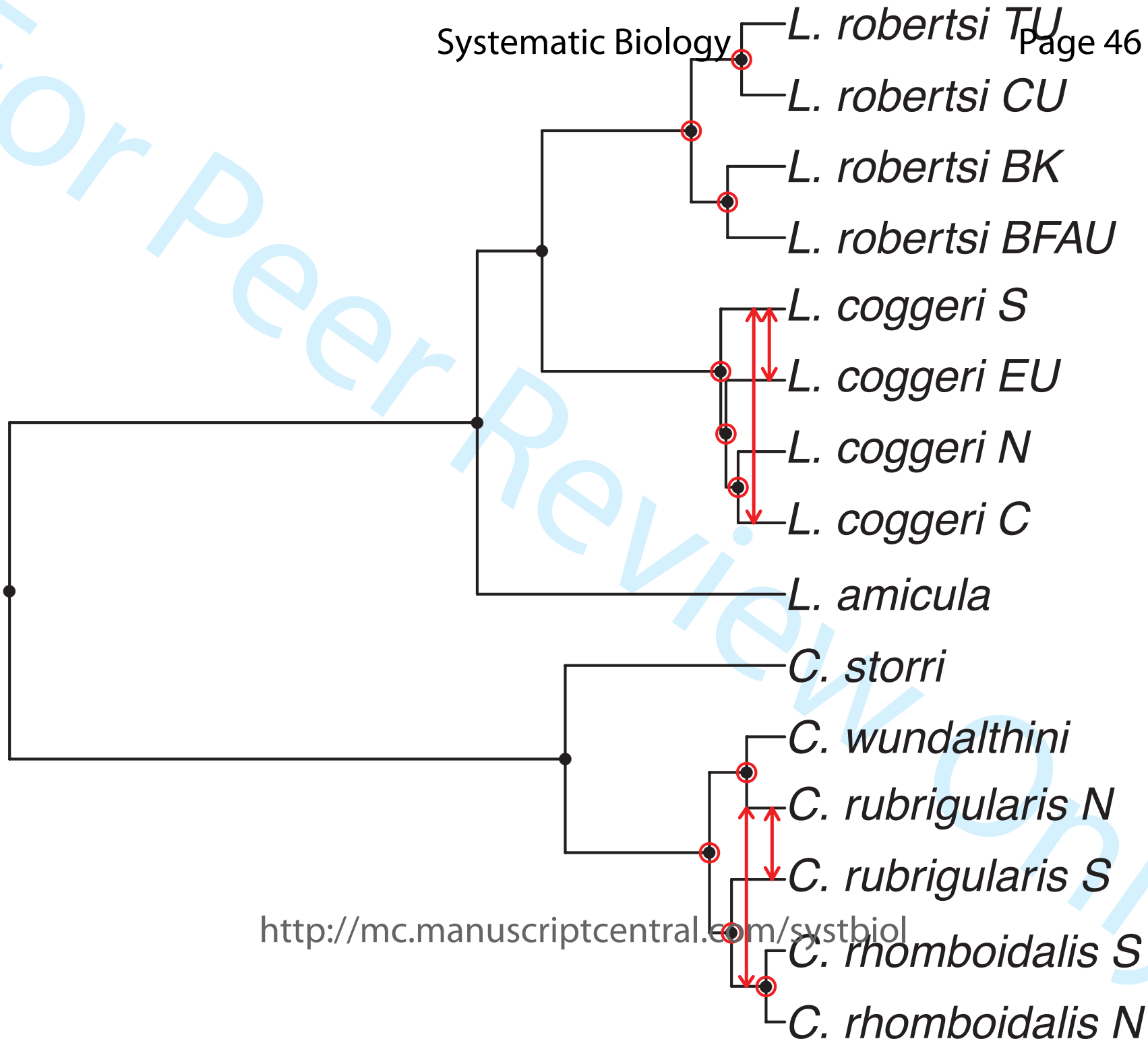

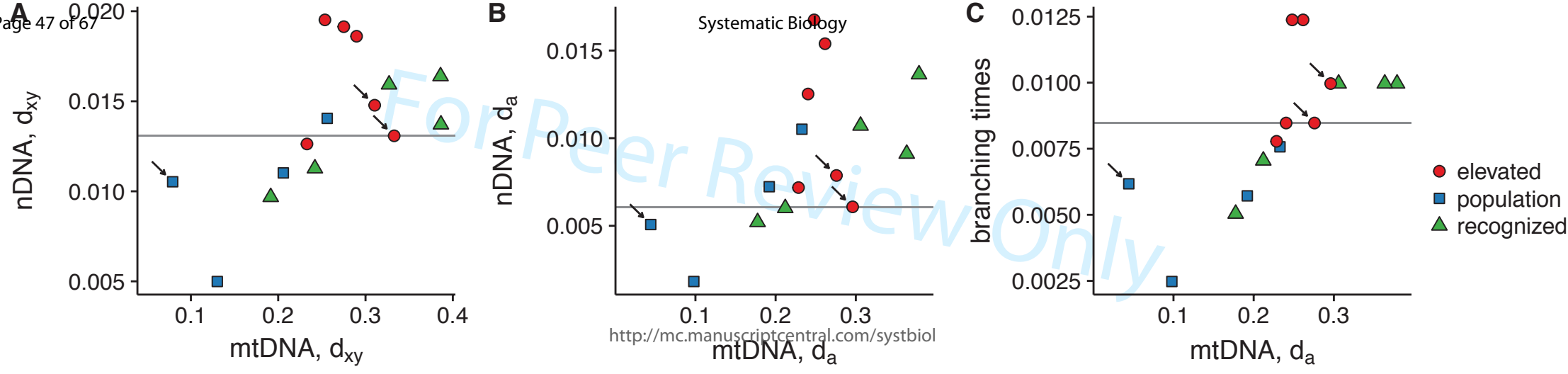

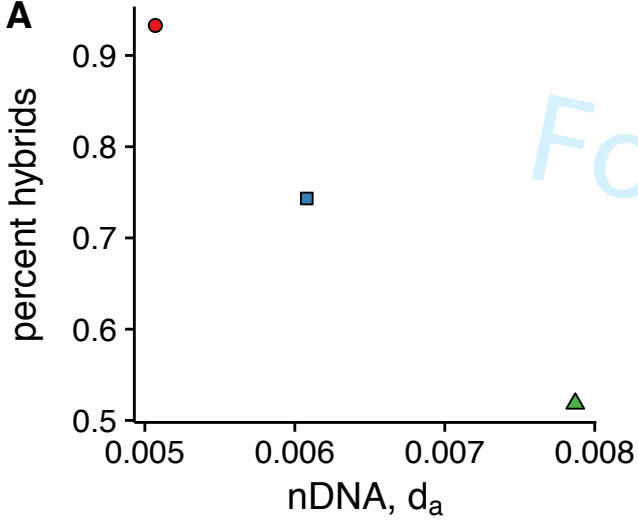

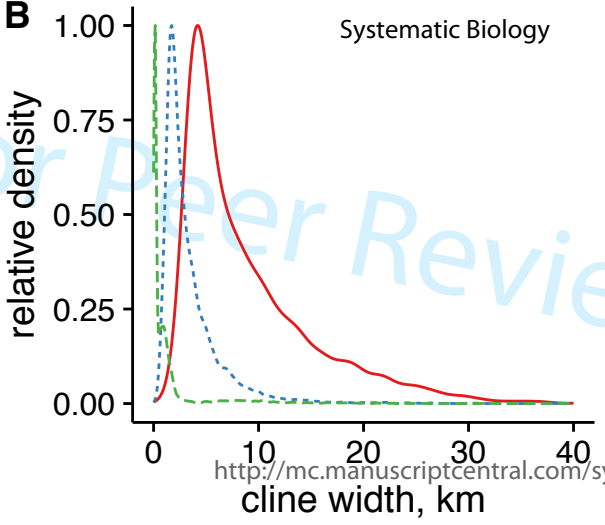

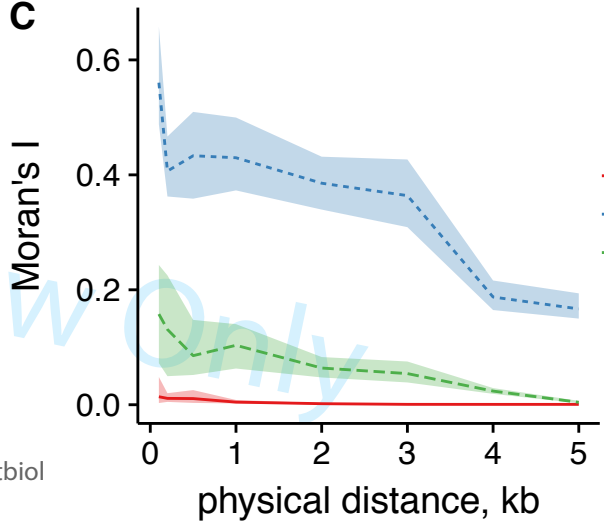

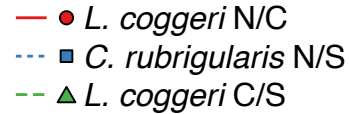

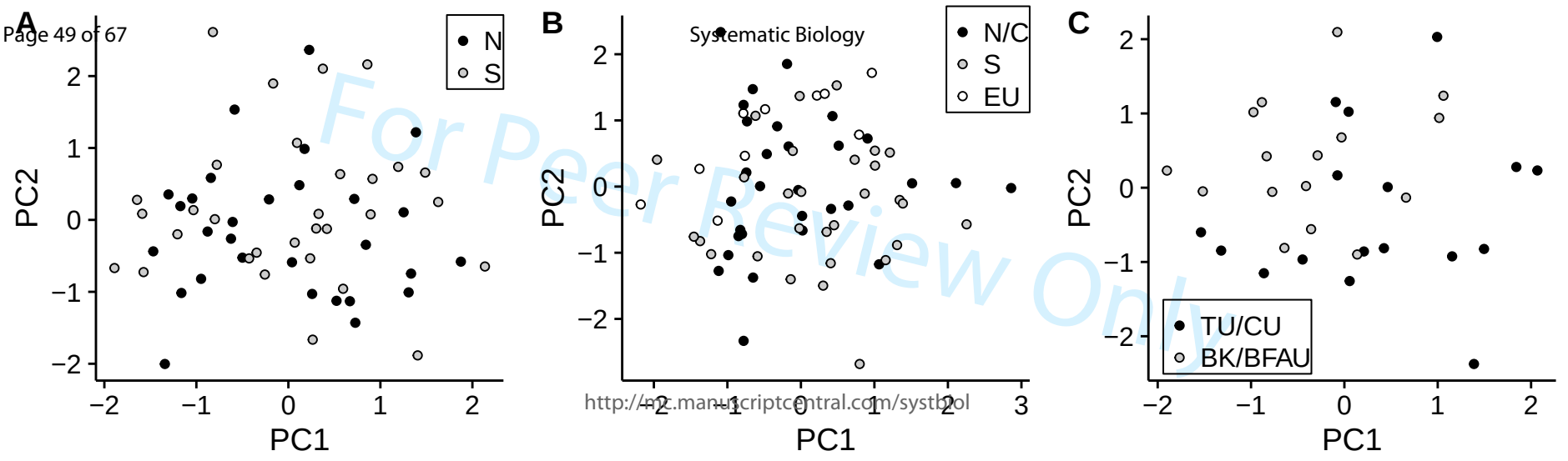

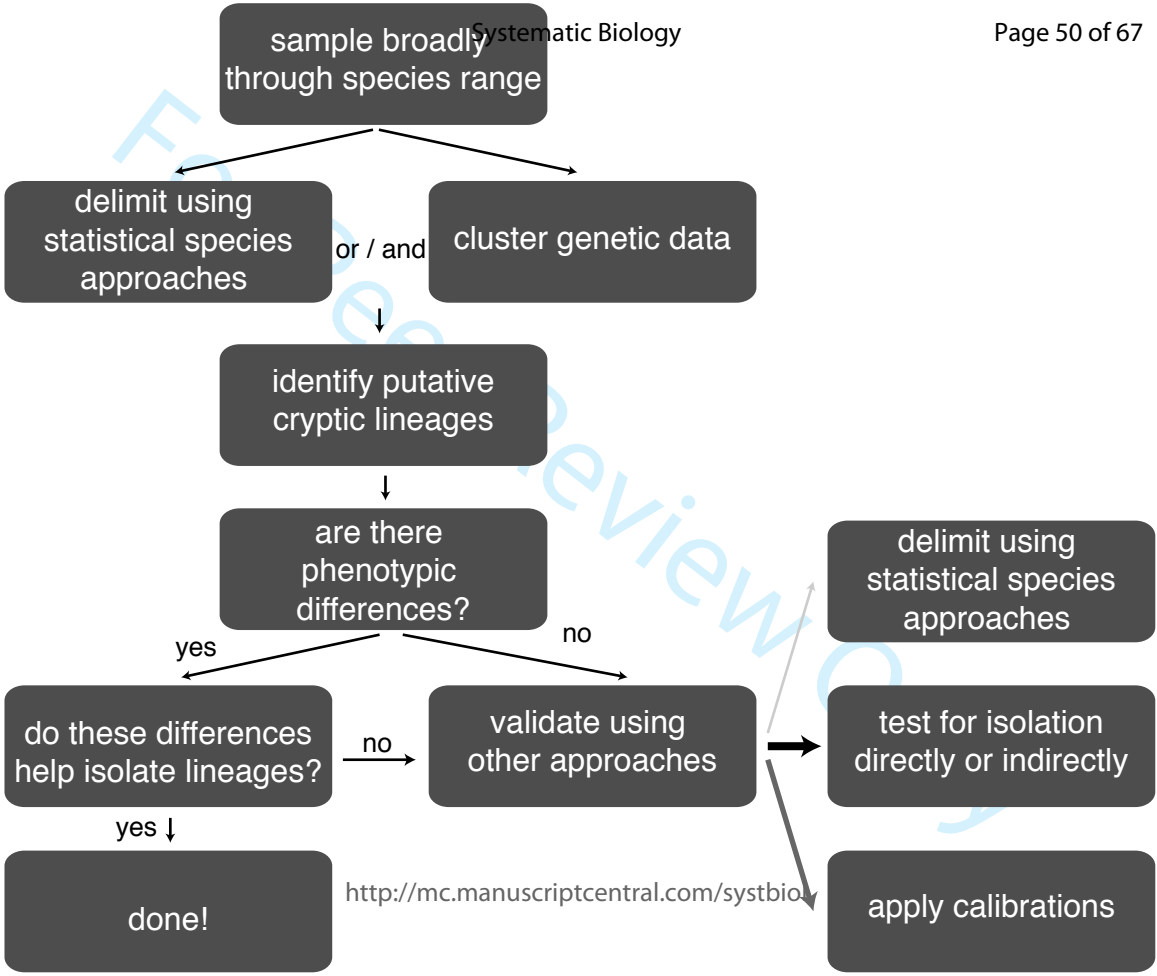

Appendix 1: Taxonomic revisions of the species groups

'Lampropholis coggeri' species group

Lampropholis coggeri Ingram

Material examined: Holotype: QM J27133 Shiptons Flat (15° 48' S, 145° 16' E). QM J60888, J60890 Big Tableland (15° 42' 30" S, 145° 16' 30" E); QM J25330 Home Rule, foot of path to Granites (15° 44' 40" S, 145° 17' 55" E); QM J25201, J25202, J25203 Granite Ck to Cedar Bay, on track (15° 45' S, 145° 20' E); QM J25254, J25255, J25271 Mt Hartley, near Home Rule, S of Cooktown (15° 46' S, 145° 19' E); QMJ57936 Mt Sampson (15° 48' S, 145° 12' E); QM J27131, J27134, Shiptons Flat (15° 48' S, 145° 16' E); QM J25217 Mt Finnigan NP (15° 48' 30" S, 145° 15' 30" E); QM J40536, J40542 Mt Finnigan, 37km S Cooktown (15° 49' S, 145° 17' E); QM J26301 Mt Finnigan, 37km S Cooktown (15° 49' 10" S, 145° 16' 50" E); QM J60886 Mt Finnigan, top grid (15° 49' 30" S, 145° 17' 30" E); QM J60221 Mt Misery Rd (15° 53' S, 145° 13' E); QM J60736 Mt Misery, ca 5km by Rd junction W/Normanby Tin works Rd (15° 53' 23" S, 145° 12' 31" E); QM J60734 Thornton Pk, N on CREB track from Daintree R (16° 06' 03" S, 145° 20' 10" E); QM J59102 Mt Windsor Tableland, Whypalla SF (16° 12' 39" S, 144° 58' 46" E); QM J48693Windsor Tableland SF, survey peg TA213 (16° 13' S, 145° E); QM J75461 Mount Windsor Tableland (16° 13' S, 145° 02' E); QM J49580 Mossman Bluff (16° 30' S, 145° 22' E); QM J49581, J49582 Bakers Blue Mt, 17km W Mt Molloy (16° 39' S, 145° 07' E); QM J39871 Bakers Blue Mt, 17km W Mt Molloy (16° 42' S, 145° 10' E); QM J55742 Kuranda (16° 49' S, 145° 38' E); QM J51952 North-South Bell Peak Saddle, Malbon Thompson Ra (17° 6' S, 145° 54' E); QM J27009 Crowley Ck, via Mt Molloy (17° 42' S, 146° 01' E).

Diagnosis: *Lampropholis coggeri* is a small, dark-sided rainforest skink with pentadactyl limbs (overlapping when adpressed) and a movable lower eyelid containing a transparent disc. It is reliably distinguished from its sibling species (*L. similis* **sp. nov.** and *L. elliotensis* **sp. nov.**) by 17 nucleotide differences in the mitochondrial gene *NADH dehydrogenase 4* that result in 15 amino acid differences among these species (Table A1).

Measurements and scale counts of holotype QM J27133: SVL 36.5 mm; AG 19.1 mm; L1 9.07 mm; L2 10.3 mm; HL 6.9 mm; HW 5.1 mm; midbody scale rows 26; paravertebral scales 48; lamellae beneath fourth toe 22; supralabials 7; infralabials 6; supraciliaries 7.

Description: SVL 32–43.6 mm (n = 30, mean = 36.3); AG % SVL 45–60% SVL (n = 30, mean = 52%); L1 24–29% SVL (n = 10, mean = 25%); L2 28–40% SVL (n = 30, mean = 34%); HW 70–83% HL (n = 31, mean = 77%). ***Body*:** Robust. Head and body continuous with almost no narrowing at neck. Snout rounded in profile. Limbs well-developed, pentadactyl, meeting or very narrowly separated when adpressed. ***Scalation:*** Dorsal scales smooth (or with three to four faint striations) with a broadly curved posterior edge; nasals widely spaced; rostral and frontonasal in broad contact; prefrontals moderately separated (narrow separation in QM J25271 and J27131); frontal contacting frontonasal, prefrontals, first two supraoculars and frontoparietal; supraoculars four, second largest; supraciliaries seven, first largest; lower eyelid movable with small palpebral disc about half the size of lower eyelid; ear opening

round or vertically elliptic, subequal to or smaller than palpebral disc; frontoparietals fused, interparietal free; primary temporal single, secondary temporals two (upper largest and overlapping lower); loreals two, subequal or second largest; preoculars two, subequal or lower largest; presuboculars two, upper largest; supralabials seven, with fifth below eye and last overlapping lower secondary temporal and postsupralabials; postsupralabial divided; infralabials six, two in contact with postmental; midbody scale rows 25–30 (n = 31, mode = 26); paravertebral scales (to the level of the posterior margin of the hindlimbs) 47–54 (n = 31, mode = 50); fourth toe longest, subdigital lamellae 20–24 (n = 30, mode = 22) with a single row of scales on the dorsal surface; outer preanal scales overlap inner preanals; three pairs of enlarged chin shields, first pair in contact, second pair separated by a single scale row, third pair separated by three scale rows.

Color pattern in preservative: *Body:* Dorsal ground color brown to olive-brown, sparsely flecked with four to six longitudinal rows of black dashes. Dorsolateral zone marked by a narrow pale stripe that extends from eye to base of tail. This is bordered below by a jagged row of black streaks or spots. Upper to mid lateral zone olive-brown with dark streaks and pale flecks, merging evenly with paler lower flanks. *Head:* As for dorsum with varying degrees of darker smudges or blotches. *Limbs:* Olive-brown with pale and dark spotting. *Tail:* As for back with continuation of the dark, broken dorsolateral stripe and bearing pale grey and black blotches on lateral surfaces. *Ventral surfaces:* Grey to cream, sparsely to heavily spotted with black. Underside of tail with dark spots on a pale background, spots often concatenated forming a reticulated pattern.

Comparison with similar species: For separating this species from other members of the '*L. coggeri*' group (*L. similis* **sp. nov.** and *L. elliotensis* **sp. nov.**), see species account for *L. similis* **sp. nov.**

Distribution: *Lampropholis coggeri* occurs north of a line extending from Mareeba, to Lake Barrine, top of the Gillies Range and Gordonvale, and then extending south-east to the mouth of the Russell River (to include the Malbon Thompson Range). The northern extent for this species is the Big Tableland area near Cooktown (Bell *et al.* 2010). The only area this species co-occurs with *L. similis* **sp. nov.** is along a narrow parapatric contact zone in the Lake Barrine–Gillies highway area. Individuals in this region require genetic verification.

Habitat and habits: Occurs in rainforest and associated moist habitats, including wet sclerophyll forests; from sea level to the uplands but is absent from the peaks where *L. robertsi* occurs (>1100 m) (Williams *et al.* 2010).

Lampropholis similis **sp. nov.**

Material examined: Holotype: QM J91380 The Pinnacles, SW of Townsville (19° 23' 42" S, 146° 39' 07" E). Paratypes: QM J49741 Gadgarra SF (17° 16' S, 145° 41' E); QM J49593 Bellenden Ker NP, TV station (17° 16' S,145° 51' E); QM J47096, J49619, J66621 Lake Eacham (17° 17' S, 145° 37' E); QM J39865 Bellenden Ker Ra, Cableway Base Station (17° 20' S, 145° 52' E); QM J45916, J45918 Russell R, cave site (17° 22' S, 145° 53' E); QM J49576, J49613 Mt Hypipamee NP (17° 25' 54" S, 145° 29' 08" E); QM J48692 Longlands Gap, Herberton Range (17° 27' 45" S, 145° 28' 30" E); QM J62904 Stone Ck, Hasenpusch Property (17° 28' S, 146° 01'

E); QM J73520 Millaa Millaa Lookout (17° 31' S, 145° 37' E); QM J61054 E margin of Palmerston NP (17° 37' S, 145° 46' E), QM J31134, J31135 Majors Mt, via Ravenshoe (17° 38' 20" S, 145° 31' 15" E); QM J62704 Dunk Is (17° 57' S, 146° 09' E); QM J74017 Kirrama (18° 10' S, 145° 38' E), QM J44199, J44173 Hinchinbrook Is, Gayundah Ck (18° 22' S, 146° 13' E); QM J49610 Curacoa Is, Palm group (18° 40' S, 146° 33' E); QM J76307 Palm Is (18° 45' S, 146° 36' E); QM J53044 Mt Halifax, 250 m SE (19° 06' S, 146° 22' E); QM J46777 Bluewater Ra, N of Townsville (19° 11' S, 146° 33' E); QM J86759 Hervey Range (19° 21' 49.98" S, 146° 28' 42.36" E); QM J91377, J91378, The Pinnacles, SW of Townsville (19° 23' 37" S, 146° 39' 07" E); QM J27621 Hervey Ra, 10km S, 35km W Townsville (19° 35' S, 146° 36' E).

Diagnosis: *Lampropholis similis* **sp. nov.** is a small, dark-sided rainforest skink with pentadactyl limbs (overlapping or very narrowly separated when adpressed) and a movable lower eyelid containing a transparent disc. It is reliably distinguished from its sibling species (*L. coggeri* and *L. elliotensis* **sp. nov.**) by 17 nucleotide differences in the mitochondrial gene *NADH dehydrogenase subunit 4* that result in 15 amino acid differences (Table A1).

Etymology: From the Latin for similar, alluding to its likeness with *L. coggeri.*

Measurements and scale counts of holotype QM J91380: SVL 39.4 mm; AG 20 mm; L1 9.58 mm; L2 14.1 mm; HL 7.9 mm; HW 6.1 mm; midbody scale rows 28; paravertebral scales 49; lamellae beneath fourth toe 22; supralabials 7; infralabials 6; supraciliaries 7.

Description: SVL 32.4–42.2 mm (n = 29, mean = 37.5); AG % SVL 41–58% SVL (n = 29, mean = 51%); L1 22–29% SVL (n = 10, mean = 25%); L2 30–39% SVL (n = 29, mean = 35%); HW 69–89% HL (n = 29, mean = 75%). ***Body*****:** Robust. Head and body continuous with almost no narrowing at neck. Snout rounded in profile. Limbs well-developed, pentadactyl, meeting or very narrowly separated when adpressed. ***Scalation:*** Dorsal scales smooth (or with three to four faint striations) with a broadly curved posterior edge; nasals widely spaced; rostral and frontonasal in broad contact; prefrontals moderately to widely separated; frontal contacting frontonasal, prefrontals, first two supraoculars and frontoparietal; supraoculars four, second largest; supraciliaries seven (eight in QM J27621), first largest; lower eyelid movable with small palpebral disc, about half the size of lower eyelid; ear opening round to vertically elliptic, subequal to or smaller than palpebral disc; frontoparietals fused, interparietal free; primary temporal single, secondary temporals two (upper largest and overlapping lower); loreals two, subequal or second largest; preoculars two, lower largest; presuboculars two (one in QMJ45916, J45918, J49613, J49741 and J66621), upper largest; supralabials seven, with fifth below eye and last overlapping lower secondary temporal and postsupralabials; postsupralabial divided; infralabials six, two in contact with postmental; midbody scale rows 26–31 (n = 29, mode = 28); paravertebral scales (to the level of the posterior margin of the hindlimbs) 47–52 (n = 29, mode = 50); fourth toe longest, subdigital lamellae 20–24 (n = 27, mode = 22) with a single row of scales on the dorsal surface; outer preanal scales overlap inner preanals; three pairs of enlarged chin shields, first pair in contact, second pair separated by a single scale row, third pair separated by three scale rows.

Color pattern in preservative: As for L. *coggeri* but some specimens from the southern portion of the range are devoid or nearly devoid of any back pattern (black dashes not present on ground color for QM J27621, J49610, J86759 and J91378).

Comparison with similar species: Separating this species from other members of the '*L. coggeri*' group (*L. coggeri* and *L. elliotensis* **sp. nov.**) relies heavily on genetic data. Seventeen nucleotide differences in the mitochondrial gene *NADH dehydrogenase subunit 4* result in differences at 15 amino acids among these species (Table A1). Additionally, both *L. similis* **sp. nov.** and *L. coggeri* tend to be longer-limbed than *L. elliotensis* **sp. nov.** (Table 2, S8). In these species, the adpressed limbs usually touch or overlap. In *L. elliotensis* **sp. nov.** the adpressed limbs are usually separated by several scale rows.

Distribution: The distribution of *L. similis* **sp. nov.** includes the Mt Bellenden Ker Range (but not the Malbon Thompson Range to the east) and extends all the way south to Hervey Range and The Pinnacles, near Townsville (Bell et al. 2010). The only area this species co-occurs with *L. coggeri* is along a narrow parapatric contact zone in the Lake Barrine–Gillies highway area. Individuals in this region require genetic verification.

Habitat and habits: Occurs in rainforest and associated moist habitats, including wet sclerophyll forests, montane heath, and gallery forests; occurs from sea level to the uplands but is generally absent from the peaks where *L. bellendenkerensis* occurs.

Lampropholis elliotensis **sp. nov.**

Material examined: Holotype: QM J91382 Mt Elliot (19° 28' 55" S, 146° 59' E). Paratypes: QM J91386, J91116 Mt Elliot (19° 28' 55" S, 146° 59' E); QM J91385 Mt Elliot (19° 28' 58" S, 146° 59' 01" E); QM J52841, J52842, J52843, J52844 Mt Elliot (19° 29' S, 146° 57' E); QM J54810, J54811, J54812, J54813, J54814, J54815, J54816, J54817 Mt Elliot, summit (19° 30' S, 146° 57' E).

Diagnosis: *Lampropholis elliotensis* **sp. nov.** is a small, dark-sided rainforest skink with pentadactyl limbs (usually separated by several scales rows when adpressed) and a movable lower eyelid containing a transparent disc (Fig. A1). It is reliably distinguished from its sibling species (*L. similis* **sp. nov.** and *L. coggeri*) by 17 nucleotide differences in the mitochondrial gene *NADH dehydrogenase subunit 4* that result in 15 amino acid differences among the species (Table A1).

Etymology: Refers to Mt Elliot, the type locality.

Measurements and scale counts of holotype QM J91382: SVL 37.5 mm; AG 19.6 mm; L1 9.26 mm, L2 12mm; HL 6 mm; HW 5.3 mm; midbody scale rows 24; paravertebral scales 48; lamellae beneath fourth toe 22; supralabials 7; infralabials 6; supraciliaries 7.

Description: SVL 31.5–40.2 mm (n = 10, mean = 36.4); AG % SVL 48–57% SVL (n = 10, mean = 53%); L1 20–26% SVL (n = 10, mean = 23%); L2 31–37% SVL (n = 10, mean = 33%); HW 75–88% HL (n = 10, mean = 80%). ***Body*:** Robust. Head and body continuous with almost no narrowing at neck. Snout rounded in profile. Limbs well-developed, pentadactyl, not meeting when adpressed (separated by several scale rows in adults). ***Scalation:*** Dorsal scales smooth (or with three to four faint striations) with a broadly curved posterior edge; nasals widely spaced; rostral and frontonasal in broad contact; prefrontals moderately to widely separated; frontal contacting frontonasal, prefrontals, first two supraoculars and frontoparietal; supraoculars four, second largest; supraciliaries seven, first largest; lower

eyelid movable with small palpebral disc, about half the size of lower eyelid; ear opening round to vertically elliptic, subequal to or smaller than palpebral disc; frontoparietals fused, interparietal free; primary temporal single, secondary temporals two (upper largest and overlapping lower); loreals two (one in QM J91385), subequal or second largest; preoculars two, subequal or lower largest; presuboculars two (only one in QM J54817 and QM J91116), upper largest; supralabials seven with fifth below eye (or eight with sixth below eye QM J52842) and last supralabial overlapping lower secondary temporal and postsupralabials; postsupralabial divided; infralabials six (rarely seven, 2/15), two in contact with postmental; midbody scale rows 24–28 (n= 14, mode = 26); paravertebral scales (to the level of the posterior margin of the hindlimbs) 48–51 (n = 14, mode = 49); fourth toe longest, subdigital lamellae 19–24 (n = 14, mode = 21) with a single row of scales on the dorsal surface; outer preanal scales overlap inner preanals; three pairs of enlarged chin shields, first pair in contact, second pair separated by a single scale row, third pair separated by three scale rows.

Color pattern in preservative: As for *L. coggeri.*

Comparison with similar species: For separating this species from other members of the '*L. coggeri*' group, see species account for *L. similis* **sp. nov.**

Distribution: Occurs on Mt Elliot, south of Townsville, in Bowling Green Bay National Park. All records come from above 600 m elevation.

Habitat and habits: Usually found amongst leaf-litter in rocky situations. This species has not been recorded in lowland rainforest around Mt Elliot, despite considerable survey effort (Hoskin, unpub. data).

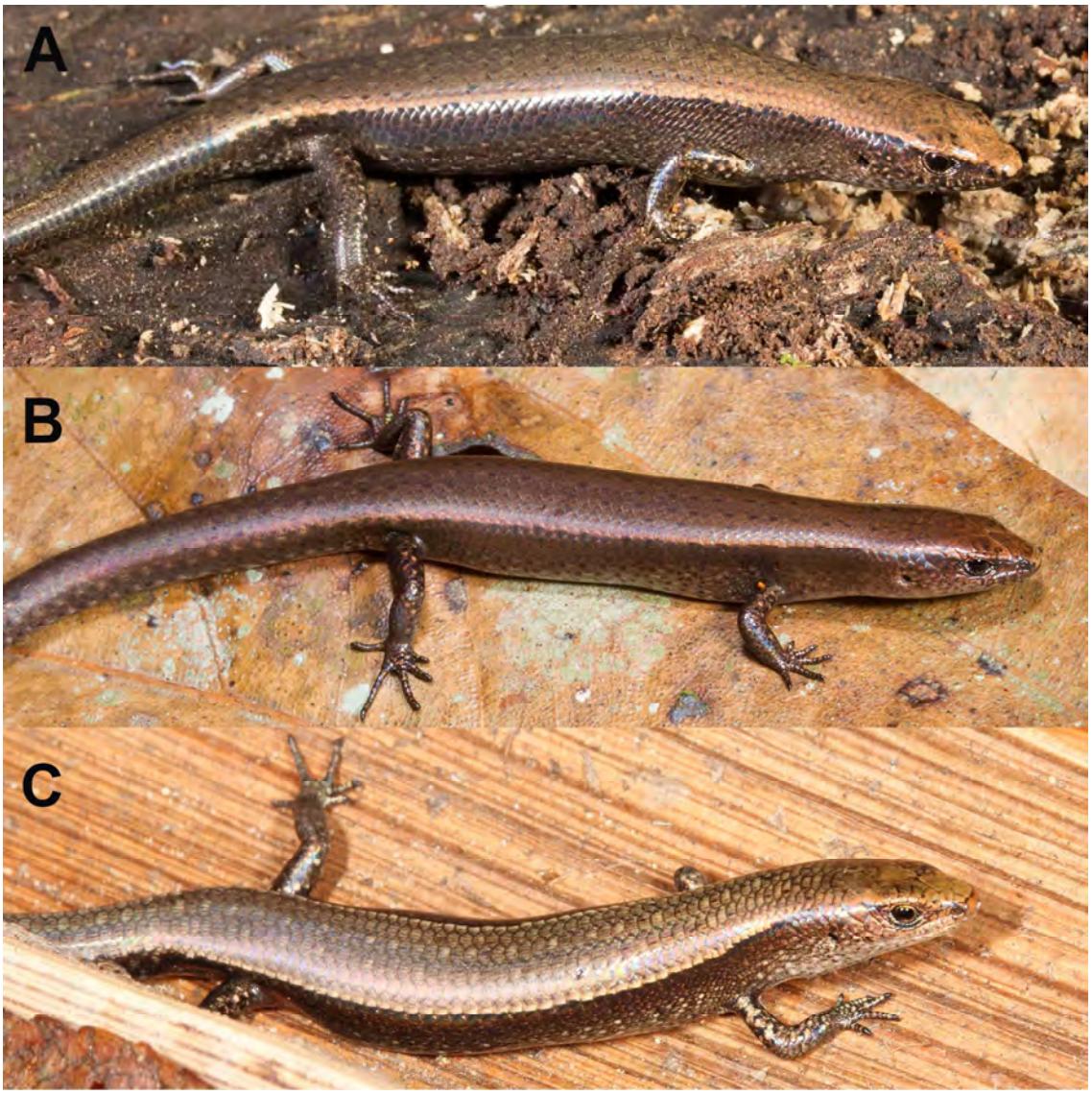

Fig. A1: (A) *Lampropholis coggeri* (Windsor Tableland, Stephen Zozaya), (B) *L. similis* **sp. nov.** (Paluma Range, Stephen Zozaya), (C) *L. elliotensis* **sp. nov.** (Mt Elliot, Conrad Hoskin).

Table A1: Diagnostic nucleotide and amino acid differences among the species in the *'Lampropholis coggeri'* species group. Nucleotide positions are given with respect to the *Scincella vandenburghi* mitochondrial genome (GenBank: NC_030776).

position	10810	10870	10894	10924	10996	11047	11215	11344, 11345	11347, 11348	11396	11424	11461	11504	11559	11569
L. similis **sp. nov.**	A I	C L	T S	G A	G G	A M	A I	A, C T	C, A H	C T	C N	A S	C S	C R	C A
L. elliotensis **sp. nov.**	C L	A I	T S	T S	A S	G V	G V	G, T V	A, A N	T I	A K	G G	C S	T C	T V
L. coggeri	C L	A I	A T	T S	G G	A M	A I	A, T I	A, G S	C T	A K	G G	T L	T C	T V

'*Lampropholis robertsi*' species group

Lampropholis robertsi Ingram

Material examined: Holotype: QM J43911 Thornton Peak, via Daintree (16° 10' S, 145° 22' E). QM J39856, J39857, J43912, J43964, J49648, J49659 Thornton Peak, via Daintree (16° 10' S, 145° 22' E); QM J43918 Thornton Peak (16° 10' S, 145° 23' E); QM J43958 Thornton Peak summit (16° 10' S, 145° 23' E); QM J55836 Mt Spurgeon, 7km N, Camp 2 (16° 22' S, 145° 13' E); QM J55833, J55834, J55835 Black Mt, 4.5km N Mt Spurgeon (16° 24' S, 145° 12' E); QM J54324 Mt Spurgeon (16° 26' S, 145° 12' E); QM J51948 Carbine Tableland, Pauls Luck (16° 27' S, 145° 15' E); QM J63545, J63548, J63550, J63553, J63561, J63563 Mt Lewis Rd, 29km along rd (16° 30' 50" S, 145° 16' 05" E); QM J47097, J48295 Mt Lewis, via Mt Molloy (16° 35' S, 145° 17' E); QM J56464 Mt Lewis (16° 35' S, 145° 17' E).

Diagnosis: A large *Lampropholis* with dark flanks and prominent spotting on the posterior ventral surfaces, a row of dark edged pale spots on underside of tail. This species is reliably distinguished from its closest congener (*L. bellendenkerensis* **sp. nov.**) by 14 nucleotide differences in the mitochondrial gene *NADH dehydrogenase 4* that result in nine amino acid differences between the species (Table A2).

Measurements and scale counts of holotype QM J43911: SVL 45.3 mm; AG 22.9; L1 12.0 mm; L2 15.9 mm; HL 8.41 mm; HW 6.0 mm; midbody scale rows 28; paravertebral scales 53; lamellae beneath fourth toe 26; supralabials 7; infralabials 6; supraciliaries 7.

Description: SVL 36.6–51.45 mm (n = 17, mean = 44.35); AG % SVL 46–54% SVL (n = 17, mean = 50%); L1 26–32% (n = 17, mean = 29%); L2 34–43% SVL (n = 17, mean = 38%); HW 69–79% HL (n = 17, mean = 73%). ***Body*:** Robust. Head and body continuous with almost no narrowing at neck. Snout rounded in profile. Limbs well-developed, pentadactyl, meeting or narrowly separated when adpressed. ***Scalation:*** Dorsal smooth (or with three to four faint striations) with a broadly curved posterior edge; nasals widely spaced; rostral and frontonasal in broad contact; prefrontals moderately to widely separated; frontal contacting frontonasal, prefrontals, first two supraoculars and frontoparietal; supraoculars four, second largest; supraciliaries seven, first usually largest but sometimes subequal to third or fourth; lower eyelid movable with small palpebral disc, less than half the size of lower eyelid; ear opening round to vertically elliptic, subequal to palpebral disc; frontoparietals fused, interparietal free; primary temporal single, secondary temporals two (upper largest and overlapping lower); loreals two, subequal or second largest; preoculars two, lower largest; presuboculars two, upper largest; supralabials seven with fifth below eye (eight in QM J55833, with sixth below eye), and last overlapping lower secondary temporal and postsupralabials; postsupralabial divided; infralabials six (seven in QM J55833 and J56464) two in contact with postmental; midbody scale rows 26–28 (n = 23, mode = 26); paravertebral scales (to the level of the posterior margin of the hindlimbs) 49–54 (n = 21, mode = 54); fourth toe longest, subdigital lamellae 21–26 (n = 21, mode = 23) with a single row of scales on the dorsal surface; outer preanal scales overlap inner preanals; three pairs of enlarged chin shields, first pair in contact, second pair separated by a single scale row, third pair separated by three scale rows.

Color pattern in preservative: Adults - *Body:* Dorsal ground color copper- brown, plain or with sparse, longitudinally aligned black dashes (intensity of color varies markedly between individuals). Striations on dorsal scales with diffuse black outlines. Dorsolateral zone with a ragged-edged black stripe that runs from behind eye to base of tail and is bordered above by a thin gold to light brown stripe. Upper lateral zone rich bronze-brown (for two to three scale rows), merging with, or clearly defined from, the paler grey to brown lower flanks which bear dark flecks and spotting. Upper and lower lateral colors may be separated by a discontinuous row of white scales (often interspersed with black streaks). *Head:* Copper-brown above with scattered dark blotches. Facial markings of varying intensity but labials often bear strong dark spots. Rostral with dark medial streak and dark lateral and lower edges**.** *Limbs:* Copper-brown with dark spotting. *Tail:* As for dorsum with darker sides bearing pale spots and a row of dark dashes on the upper lateral edge (a broken continuation of dark dorsolateral stripe) *Ventral surfaces:* Grey with varying degrees of spotting sometimes present on chin and throat but most prominent on lower body, hindlimbs and tail. A row of dark-edged, pale blotches on underside of tail. **Juveniles:** Ventral pattern bold. Infralabials barred and dark speckling present on chin, throat and body. Underside of body dark with prominent white blotches. Large pale spots along underside of tail.

Comparison with similar species: *Lampropholis robertsi* and *L. bellendenkerensis* **sp. nov.** cannot be separated using morphological characters. They are distinguished genetically by 13 nucleotide differences in the mitochondrial gene *NADH dehydrogenase 4* that result in nine amino acid differences between the two species (Table A2).

Distribution: *Lampropholis robertsi* is restricted to Thornton Peak and the uplands of the Carbine Tableland (e.g., Mt Lewis, Mt Spurgeon).

Habitat and habits: Occurs in upland rainforest and heath (all records come from above approximately 900 m elevation). Most often seen in warmer, sunlit areas such as in canopy gaps or rocky areas.

Lampropholis bellendenkerensis **sp. nov.**

Material examined: Holotype: QM J39855 Bellenden Ker Ra (17° 20' S, 145° 52' E). Paratypes: QM J51406 Mt Lewis SF, 25 km along rd (16° 31' 45" S, 145° 16' 30" E); QM J62209 Bellenden Ker, top of (17° 13' S, 145° 53' E); QM J55837 Massey Ra, 4km W Centre Bellenden Ker (17° 16' S, 145° 49' E); QM J40033, J40036, J40037, J40038, J40039 Mt Bellenden Ker summit, near TV Tower and station (17° 16' S, 145° 51' E); QM J46193 Bellenden Ker NP (17° 16' S, 145° 51' E); QM J39490, J39491 Mt Bellenden Ker summit (17° 20' S, 145° 52' E); QM J40041 Mt Bartle Frere, east face (17° 24' S, 145° 49' E); QM J47956, J47959 Mt Bartle Frere (17° 24' S, 145° 49' E); QM J64652 Longlands Gap (17° 28' S, 145° 29' E); QM J31196 Mt Fisher, via Millaa Millaa (17° 33' S, 145° 33' E); QM J41707, J41708 Mt Fisher, Whiteing Rd, 7 km SW Millaa Millaa (17° 33' S, 145° 33' E).

Diagnosis: A large *Lampropholis* with dark flanks and prominent spotting on the posterior ventral surfaces, a row of dark edged pale spots on underside of tail (Fig. A2). This species is reliably distinguished from its closest congener (*L. robertsi*) by 13 nucleotide differences in

the mitochondrial gene *NADH dehydrogenase 4* that result in nine amino acid differences between the species (Table A2).

Etymology: Refers to Mt Bellenden Ker, the type locality.

Measurements and scale counts of holotype QM J39855: (specimen also a paratype of *L. robertsi*)**:** SVL 43.7mm; AG 22.9 mm; L1 12.1 mm; L2 16.6 mm; HL 8.1 mm; HW 6.1 mm; midbody scale rows 28; paravertebral scales 54; lamellae beneath fourth toe 23; supralabials 7; infralabials 6; supraciliaries 7.

Description: SVL 35.4–47.5 mm (n = 16, mean = 42.13); AG % SVL 46–56% SVL (n = 16, mean = 51%); L1 24–30% (n = 16, mean = 28); L2 33–40% SVL (n = 16, mean = 37%); HW 67–75% HL (n = 16, mean = 71%). ***Body*****:** Robust. Head and body continuous with almost no narrowing at neck. Snout rounded in profile. Limbs well-developed, pentadactyl, meeting or narrowly separated when adpressed. ***Scalation:*** Dorsal scales smooth (or with three to four faint striations) with a broadly curved posterior edge; nasals widely spaced; rostral and frontonasal in broad contact; prefrontals moderately to widely separated; frontal contacting frontonasal, prefrontals, first two supraoculars and frontoparietal; supraoculars four, second largest; supraciliaries seven (eight in QM J47959, J46193 and J51406), first largest but sometimes subequal to third or fourth; lower eyelid movable with small palpebral disc, less than half the size of lower eyelid; ear opening round to vertically elliptic, subequal to or smaller than palpebral disc; frontoparietals fused, interparietal free; primary temporal single, secondary temporals two (upper largest and overlapping lower); loreals two, subequal or second largest; preoculars two, lower largest; presuboculars two, upper largest; supralabials seven, with fifth below eye and last overlapping lower secondary temporal and postsupralabials; postsupralabial divided; infralabials six, two in contact with postmental; midbody scale rows 26–30 (n = 18, mode = 28); paravertebral scales (to the level of the posterior margin of the hindlimbs) 48–55 (n = 17, mode = 51); fourth toe longest, subdigital lamellae 21–24 (n = 15, mode = 23) with a single row of scales on the dorsal surface; outer preanal scales overlap inner preanals; three pairs of enlarged chin shields, first pair in contact, second pair separated by a single scale row, third pair separated by three scale rows.

Color pattern in preservative: As for *L. robertsi.*

Comparison with similar species: See species account for *L. robertsi.*

Distribution: *Lampropholis bellendenkerensis* **sp. nov.** occurs in the uplands of the Bellenden Ker Range (Mt Bellenden Ker and Mt Bartle Frere) and in the highest areas of the southern Atherton Tablelands (including Mt Baldy, Longman's Gap, Mt Fisher and the Tully Falls area). All records come from above approximately 900 m elevation.

Habitat and habits: As for *L. robertsi.*

Fig. A2: (A) *Lampropholis robertsi* (Mt Lewis, Stephen Zozaya) (B) *L. bellendenkerensis* **sp. nov.** (Mt Bartle Frere, Anders Zimny).

Table A2: Diagnostic nucleotide and amino acid differences among the species in the '*Lampropholis robersti*' species group. Nucleotide positions are given with respect to the *Scincella vandenburghi* mitochondrial genome (GenBank: NC_030776).

position	**10863**	**11014**			**11287 - 9**		**11302, 11304**		**11347**		**11364**		**11380, 11382**		**11468**		**11504**	
L. robertsi	A/G	M	G	A	ACG	T	G, T	V	A	N	A	Q	C, C	L	T	M	T	L
***L. bellendenkerensis* sp. nov.**	T	I	A	T	TTA	L	A, C	I	G	D	C	H	A, T	I	C	T	C	S

'*Carlia rubrigularis*' species group

Carlia rubrigularis Ingram & Covacevich

Material examined: Holotype: QM J29956 Innisfail, NE Queensland (17° 32' S, 146° 01' E). Paratypes: QM J50463 Lake Eacham (17° 16' 57" S, 145° 37' 46" E); QM J50466 Lake Eacham (17° 17' S, 145° 38' E); QM J45919 Malanda (17° 21' S, 145° 36' E); QM J71004 Boonjee, 6.5km ESE Lamin's Hill (17° 25' 30" S, 145° 44' 30" E); QM J55865 Polly Ck, Seymour Ra (17° 28' S, 146° 02' E); QM J48167, J48169 Walter Hill Ra, Charappa Ck drainage, Suttees Rd (17° 42' 30" S, 145° 41' 30" E); QM J50459 Cochable Ck, plateau logging area (17° 44' S, 145° 39' E); QM J50458 Cochable Ck, plateau logging area (17° 44' S, 145° 47' E); QM J71002 Murdering Pt, Kurrimine Bch, via Silkwood. (17° 46' 30" S, 146° 06' 30" E); QM J48206 Billy Ck Bridge SF 758, vicinity of bridge (17° 49' 25" S, 145° 47' 05" E); QM J73365 Koombooloomba township (17° 50' S, 145° 34' E); QM J48175 Laceys Ck SF, Mission Beach (17° 51' 10" S, 146° 03' 55" E); QM J30835 Mission Beach (17° 52' S, 146° 06' E); QM J70987 Tully, 15km E (17° 56' S, 146° 03' E); QM J65366 Kirrama Ra (18° 03' 30" S, 145° 36' 30" E); QM J48374 Kirrama SF, Jennings Logging Area (18°04' 30" S, 145° 37' 30" E); QM J48315 Kirrama Ra, Alma Gap Logging Rd (18° 12' 15" S, 145° 49' 30" E); QM J48336 Kirrama Ra, crest of range rd (18° 13' 30" S, 145° 47' 30" E); QM J44191, J44215 Hinchinbrook Is, Gayundah Ck (18° 22' S, 146° 13' E); QM J61207 Broadwater Ck NP, 11km S of Mt McAlister (18° 23' 30" S, 145° 56' 30" E); QM J45549 Mt Diamantina (18° 25' S, 146° 17' E); QM J51591 Long Pocket, Herbert R (18° 31' S, 146°00' E), QM J75285 Paluma (18° 57' S, 146° 09' E); QM J79575, J79652 Mt Spec (18° 57' S, 146° 11' E); QM J79600, J79602 Paluma (19° 00' S, 146° 12' E); QM J74902 Bluewater Ra, N of Townsville (19° 14' 30" S, 146° 24' 30" E).

Diagnosis: *Carlia rubrigularis* is distinguished from all other *Carlia spp*., except members of the '*C. rhomboidalis*' group, in possessing an interparietal fused to the frontoparietals. As with *C. crypta* **sp. nov.,** adult males possess a red throat. It is reliably distinguished from this species by four nucleotide differences in the mitochondrial gene *NADH dehydrogenase subunit 4* that result in three amino acid differences (Table A3).

Measurements and scale counts of holotype QM J29956: SVL 40.7 mm; AG 20.8 mm; L1 14.8 mm; L2 20.5 mm; HL 9.5 mm; HW 7.2 mm; midbody scale rows 32; paravertebral scales 44; lamellae beneath fourth toe 29; supralabials 7 ; infralabials 6 ; supraciliaries 7.

Description: SVL 40.7–55.3 mm (n = 31, mean = 48.7); AG % SVL 42–55% SVL (n = 31, mean = 49%); L1 33–36% (n = 10, mean = 35%); L2 41–50% SVL (n = 31, mean = 45%); HW 68–88% HL (n = 31, mean = 74%). ***Body*:** Robust. Head and body continuous with almost no narrowing at neck. Snout rounded in profile. Limbs well-developed, forelimb tetradactyl, hindlimb pentadactyl, limbs broadly overlapping when adpressed. ***Scalation:*** Dorsal scales smooth (with three to four faint striations) with a broadly curved posterior edge; nasals widely spaced; rostral and frontonasal in broad contact; prefrontals large, narrowly to moderately separated; frontal contacting frontonasal, prefrontals, first two supraoculars and frontoparietal; supraoculars four, second largest; supraciliaries seven (eight in QM J55865 and J30835), first largest but sometimes subequal to fourth; lower eyelid movable with a small palpebral disc, less than or equal to half the size of lower eyelid; ear opening round

with one to three enlarged, pointed lobules on anterior margin and smaller pointed lobules on other margins, larger than palpebral disc; frontoparietals and interparietal fused forming a single shield; primary temporal single, secondary temporals two (upper largest and overlapping lower); loreals two, second usually largest but sometimes subequal; preoculars two, lower largest; presuboculars one; supralabials seven, with fifth below eye (eight with sixth below eye in QM J79575) and last overlapping lower secondary temporal and postsupralabials; postsupralabial divided; infralabials six, two in contact with postmental; midbody scale rows 30–36 (n = 31, mode = 32); paravertebral scales (to the level of the posterior margin of the hindlimbs) 45–50 (n = 31, mode = 45); fourth toe longest, subdigital lamellae 24–31 (n = 31, mode = 29) with a single row of scales on the dorsal surface; outer preanal scales overlap inner preanals; three pairs of enlarged chin shields, first pair in contact, second pair separated by a single scale row, third pair separated by three scale rows.

Color pattern in preservative: Adults: *Body:* Dorsum olive-brown with fine black striations. Usually a row of dark paravertebral spots or streaks extending from axilla to groin, with an unmarked scale separating each spot (some specimens with more extensive spotting, spots present on all dorsal rows). A narrow pale stripe is present on the dorsolateral zone, running from behind eye, onto dorsal edges of tail. Upper lateral surfaces copper-brown, infused with black and bearing dark-edged scales. Some indication of a pale, dark-edged, mid-lateral line or row of spots is usually present but not always discernible (strongest posterior to ear). Lower flanks light brown to grey, merging evenly with pale ventral color. *Head:* Copper colored, usually plain but sometimes a few small darker markings are present. A dark streak present beneath eye, along anterior orbit. *Limbs:* Copper-brown with dark speckling. *Tail:* As for dorsum with a dark transverse streak along the anterior edge of every second vertebral scale. *Ventral surfaces:* Cream to silvery grey. J**uveniles:** As for adults but pattern stronger and more sharply defined particularly the dorsolateral and mid lateral stripes. The latter branches and extends as a pale, dark-edged streak onto the upper surfaces of the fore and hindlimbs.

In life: Red on throat and neck of breeding males.

Comparison with similar species: For separating this species from other members of the '*C. rugrigularis*' group, see species account for *C. crypta* **sp. nov.**

Distribution: See species account for *C. crypta* **sp. nov.**

Habitat and habits: See species account for *C. crypta* **sp. nov.**

***Carlia crypta* sp. nov.**

Material examined: Holotype: QM J75457 Mt Lewis SF, Forestry clearing (16° 35' 40" S, 145° 16' 27" E). Paratypes: QM J25141 Home Rule, near Home Rule Falls, S of Cooktown (15° 44' S, 145° 18' E); QM J25240, J25242 Mt Hedley slopes (15° 44' S, 145° 16' E); QM J25146 Home Rule, Mt Hedley Spur (15° 44' S, 145° 17' E); QM J50335 Home Rule (15° 44' S, 145° 17' E); QM J25293 Home Rule Falls, near (15° 44' S, 145° 18' E); QM J25198, J25199, J25200 Granite Ck to Cedar Bay, on track (15° 45' S, 145° 20' E); QM J25247, J25249 Mt Hartley, near Home Rule, S of Cooktown (15° 46' S, 145° 19' E); QM J17906 Shiptons Flat, Parrot Ck, 32– 48 km S

Cooktown (15° 48' S, 145° 15' E); QM J17901, J24649, J24807 Shiptons Flat, via Cooktown (15° 48' S, 145° 16' E); QM J25296 12 Mile Scrub, Gap Ck (15° 48' 30" S, 145° 19' 30" E); QM J25209 Mt Finnigan NP, Horan Ck (15° 49' 10" S, 145° 16' 50" E); QM J75102, J75287 McDowall Range (16° 06' S, 145° 20' E); QM J50482 Windsor Tableland (16° 11' S, 145° 05' E); QM J64965 Windsor Tableland (16° 13' S, 144° 59' E); QM J92870 Daintree (16° 15' S,145° 19' E); QM J54459 Mt Spurgeon 16° 26' S, 145° 12' E); QM J55832 Mt Spurgeon, 2.5km S (16° 28' S, 145° 12' E); QM J51564 Mossman Bluff Track, 5–10km W Mossman (16° 28' S, 145° 17' E); QM J50465 Mossman Gorge NP (16° 28' S, 145° 20' E); QM J54353 Mossman (16° 28' S, 145° 23' E); QM J89877 Black Mountain Rd, Hockley (16° 36' 41" S, 145° 27' 09" E).

Diagnosis: *Carlia crypta* **sp. nov.** is distinguished from all other *Carlia spp*., except other members of the '*C. rubrigularis*' group, in possessing an interparietal fused to the frontoparietals. As with *C. rubrigularis*, adult males possess a red throat. It is reliably distinguished from this species by four nucleotide differences in the mitochondrial gene *NADH dehydrogenase subunit 4* that result in three amino acid differences (Table A3).

Etymology: From the Latin for hidden, referring to its morphological similarity with *C. rubrigularis*.

Measurements and scale counts of holotype QM J75457: SVL 47.5mm; AG 24.1 mm; L1 14.4 mm; L2 21.2 mm; HL 10 mm; HW 8.4 mm; midbody scale rows 32; paravertebral scales 44; lamellae beneath fourth toe 29; supralabials 7; infralabials 6; supraciliaries 7.

Description: SVL 43.9–54.4 mm (n = 29, mean = 48.4); AG % SVL 41–54% SVL (n = 29, mean = 48%); L1 40–51% (n = 29, mean = 45%); L2 40–51% SVL (n = 29, mean = 45%); HW 67–85% HL (n = 29, mean = 77%). ***Body*:** Robust. Head and body continuous with almost no narrowing at neck. Snout rounded in profile. Limbs well-developed, forelimb tetradactyl, hindlimb pentadactyl, broadly overlapping when adpressed. ***Scalation:*** Dorsal scales smooth (with three to four faint striations) with a broadly curved posterior edge; nasals widely spaced; rostral and frontonasal in broad contact; prefrontals large, narrowly to moderately separated; frontal contacting frontonasal, prefrontals, first two supraoculars and frontoparietal; supraoculars four, second largest; supraciliaries seven, first usually largest but sometimes subequal to fourth; lower eyelid movable with a small palpebral disc, less than or equal to half the size of lower eyelid; ear opening round with one to three enlarged, pointed lobules on anterior margin and smaller pointed lobules on other margins, larger than palpebral disc; frontoparietals and interparietal fused forming a single shield; primary temporal single, secondary temporals two (upper largest and overlapping lower); loreals two, second usually largest; preoculars two, lower largest; presuboculars one; supralabials seven, with fifth below eye and last overlapping lower secondary temporal and postsupralabials; postsupralabial divided; infralabials six, two in contact with postmental; midbody scale rows 28–34 (n = 29, mode = 32); paravertebral scales (to the level of the posterior margin of the hindlimbs) 43–47 (n = 29, mode = 44); fourth toe longest, subdigital lamellae 26–33 (n = 28, mode = 29) with a single row of scales on the dorsal surface; outer preanal scales overlap inner preanals; three pairs of enlarged chin shields, first pair in contact, second pair separated by a single scale row, third pair separated by three scale rows.

Color pattern in preservative: Variable, as for *C. rubrigularis*.

In life: Red on throat and neck of breeding males.

Comparison with similar species: *Carlia crypta* **sp. nov.** can only be confused with other members of the '*C. rubrigularis*' group (*C. wundalthini* Hoskin, *C. rubrigularis* Ingram & Covacevich and *C. rhomboidalis* Peters). It is readily separated from both *C. wundalthini* and *C. rhomboidalis* by the coloration of adult males (throat red *vs.* throat pale in *C. wundalthini* and throat red and blue in *C. rhomboidalis*). It is further separated from *C. wundalthini* in lacking an orange flush on the neck and flanks (*vs.* orange flush present). In both *Carlia crypta* **sp. nov.** and *C. rubrigularis*, adult males possess red throats and have no breeding coloration on the flanks. These species cannot be separated by morphological characters or color pattern differences and are diagnosed by genetic data instead. Four nucleotide differences in the mitochondrial gene NADH dehydrogenase 4 lead to three amino acid differences that reliably distinguish the two species (Table A3).

Further, in most instances, these species can be distinguished in the field by their distributions. *Carlia crypta* occurs north of a diagonal line running from approximately Mareeba, through Lake Tinaroo, along the spine of the Lamb Range uplands, to southern Cairns, and east of a line running from southern Cairns to the mouth of the Russell River (i.e. to include Malbon Thompson Range) (Phillips et al. 2004; Dolman & Moritz 2006). The northern limit for *C. crypta* is the Big Tableland area near Cooktown. *Carlia rubrigularis* occurs south of the line defined above, with its southern extent at Pattersons Gorge at the far southern end of Paluma Range, near Townsville. The only area where these species co-occur is a narrow parapatric zone along the approximate boundary defined above. Individuals found along this contact zone (e.g., around Lake Tinaroo, the uplands of Lamb Range, Copperload Dam region, southern Cairns, Redlynch area) require genetic verification.

Distribution: As defined in the paragraph above.

Habitat and habits: Occurs in rainforest and associated moist habitats, including wet sclerophyll forest and montane heath; from sea level to the uplands, but typically absent from the highest peaks.

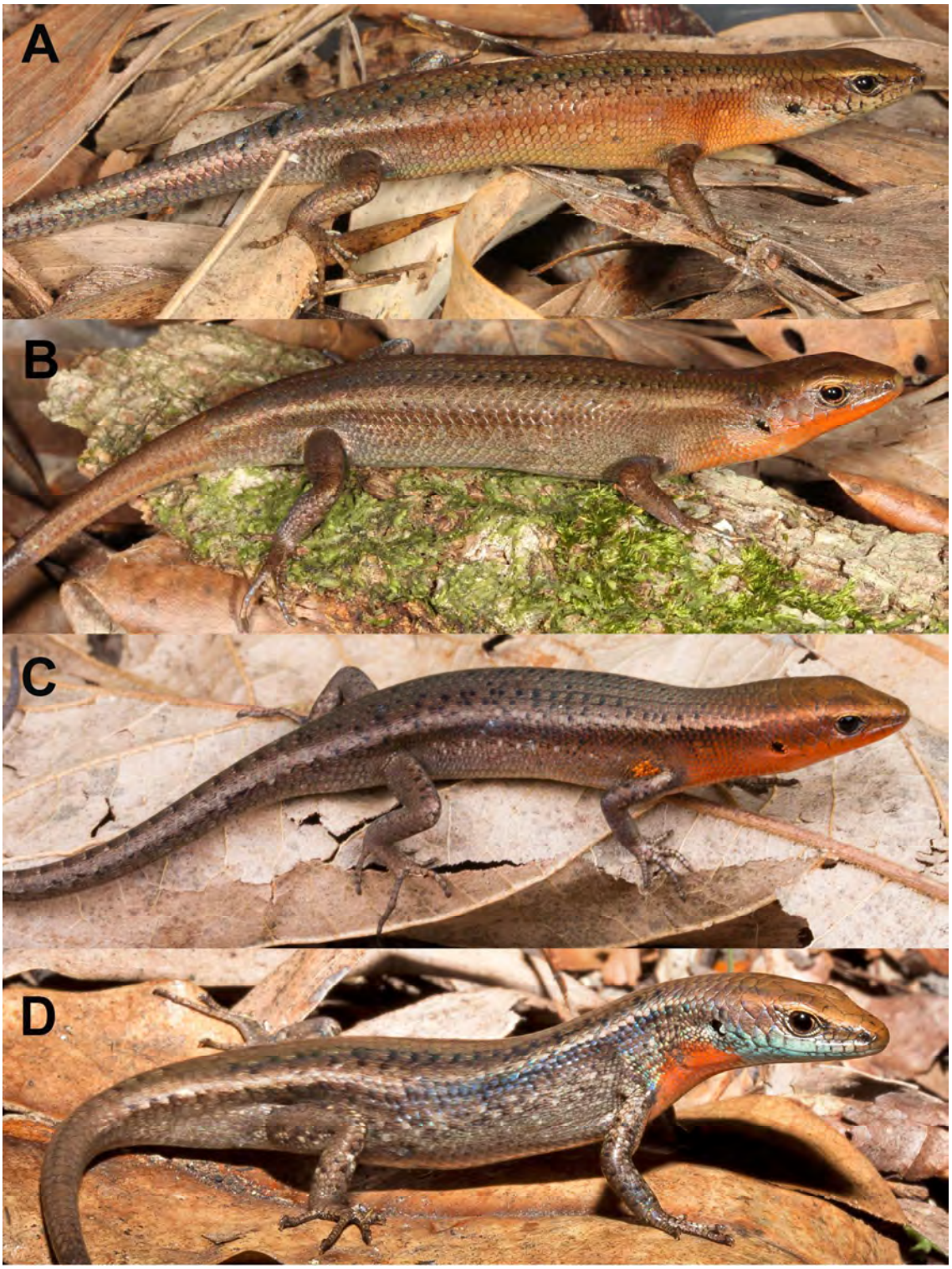

Fig. A3: Pictures of males in breeding color: (A) *Carlia wundalthini* (Cape Melville, Conrad Hoskin), (B) *C. crypta* **sp. nov**. (Mt Lewis, Conrad Hoskin), (C) *C. rubrigularis* (Kirrama Range, Stephen Zozaya), (D) *C. rhomboidalis* (Mt Blackwood, Anders Zimny). *C. rhomboidalis* and *C. wundalthini* are morphologically distinct from the other species in both breeding colors and body shape (Hoskin 2014, Dolman 2008).

Table A3: Diagnostic nucleotide and amino acid differences among the species in the *'Carlia rubrigularis'* species group. Nucleotide positions are given with respect to the *Scincella vandenburghi* mitochondrial genome (GenBank: NC_030776).

position	**11344, 11345**		**11434**		**11450**	
C. wundalthini	G, C	A	A	I	T	M
***C. crypta* sp. nov.**	G, C	A	G	V	T	M
C. rubrigularis	A, T	I	A	I	C	T
C. rhomboidalis	A, C	T	A	I	T	M

Table A4: Summary of characters across the seven species studied for morphology and scales, including the range seen, the number of individuals measured, and the mean or modal value.

	Lampropholis					***Carlia***	
Character	*coggeri*	*similis* **sp. nov.**	*elliotensis* **sp. nov.**	*robertsi*	*bellendenkerensis* **sp. nov.**	*rubrigularis*	*crypta* **sp. nov.**
SVL (mm)	32–44 n 30 mean 36	32–42 n 29 mean 38	32–40 n 10 mean 36	37–51 n 17 mean 44	35–48 n 16 mean 42	41–55 n 31 mean 49	44–54 n 29 mean 48
AG %SVL	45–60% n 30 mean 52%	41–58% n 29 mean 51%	48–57% n 10 mean 53%	46–54% n 17 mean 50	46–56% n 16 mean 51%	42–55% n 31 mean 49%	41–54% n 29 mean 48%
HW % HL	70–83% n 31 mean 77%	69–89% n 29 mean 75%	75–88% n 10 mean 80%	69–79% n17 mean 73%	67–75% n 16 mean 71%	68–88% n 31 mean 74%	67–85% n 29 mean 77%
L1 % SVL	24–29% n 10 mean 25%	22–29% n 10 mean 25%	20–26% n 10 mean 23%	26–32% n 17 mean 29%	24–30% n 16 mean 28%	33–36% n 10 mean 35%	30–38% n 10 mean 34%
L2 % SVL	28–40% n 30 mean 34%	30–39% n 29 mean 35	31–37% n 10 mean 33%	34–43% n 17 mean 38%	33–40% n 16 mean 37%	41–50% n 31 mean 45%	40–51% n 29 mean 45%
Midbody scale rows	25–30 n 31 mode 26	26–31 n 29 mode 28	24–28 n 14 mode 26	26–28 n 23 mode 26	26–30 n 18 mode 28	30–36 n 31 mode 32	28–34 n 29 mode 32
Paravertebral scales	47–54 n 31 mode 50	47–52 N 29 mode 50	48–51 n 14 mode 49	49–54 n 21 mode 54	48–55 n 17 mode 51	45–50 n 31 mode 45	43–47 n 29 mode 44
Subdigital lamellae 4th toe	20–24 n 30 mode 22	20–24 n 27 mode 22	19–24 n 14 mode 21	21–26 n 21 mode 23	21–24 n 15 mode 23	24–31 n 31 mode 29	26–33 n 28 mode 29

REFERENCES

Williams, S., VanDerWal, J., Isaac, J., Shoo, L.P., Storlie, C., Fox, S., Bolitho, E.E., Moritz, C., Hoskin, C.J. and Williams, Y.M., 2010. Distributions, life history specialisation, and phylogeny of the rainforest vertebrates in the Australian Wet Tropics. *Ecology* (91): 2493.

Data file(s):
Supplementary Tables & Figures

Thank you for submitting your data package to Dryad for journal review. Please read the following information carefully and save it for future reference.

(1) Your data package is temporarily available to journal editors and reviewers via a private review link (see below).

(2) It has been assigned a Digital Object Identifier (DOI), but this DOI will not work until/unless your manuscript is accepted for publication and your data package is approved by our curators.

(3) If/when your manuscript is accepted, please make sure that the DOI, and NOT the review link, is included in the published article. More information about citing your data is below.

(4) If you need to modify your submission, please see the instructions below. Do not create multiple Dryad submissions associated with the same manuscript.

(5) If you were asked to enter a credit card number, your card will not be charged unless/until your manuscript is accepted and your submission is approved. You will receive a confirmation when your card is charged.

YOUR TEMPORARY REVIEW LINK:

http://datadryad.org/review?doi=doi:10.5061/dryad.g7v1b

(for journal access prior to manuscript acceptance only, DO NOT link in your manuscript)

YOUR DRYAD DOI:

doi:10.5061/dryad.g7v1b

(for inclusion in the published article)